

THE EPITAXIAL GROWTH OF SELENIUM  
ON IONIC SUBSTRATES

By

R. H. C. LIBRARY	
CLASS	<sup>T</sup> BPTJ
No.	Gri
ACC. No.	100,740
DATE ACQ	July '71

C.H. Griffiths, B.Sc.

A thesis submitted for the degree of  
Master of Science in the University of London

Department of Physics,  
Royal Holloway College.

August, 1963.

ProQuest Number: 10096397

All rights reserved

INFORMATION TO ALL USERS

The quality of this reproduction is dependent upon the quality of the copy submitted.

In the unlikely event that the author did not send a complete manuscript and there are missing pages, these will be noted. Also, if material had to be removed, a note will indicate the deletion.



ProQuest 10096397

Published by ProQuest LLC(2016). Copyright of the Dissertation is held by the Author.

All rights reserved.

This work is protected against unauthorized copying under Title 17, United States Code.  
Microform Edition © ProQuest LLC.

ProQuest LLC  
789 East Eisenhower Parkway  
P.O. Box 1346  
Ann Arbor, MI 48106-1346

ACKNOWLEDGEMENTS

I wish to thank Dr. C. S. Heavens for his guidance, help, and advice throughout this work, and Dr. R. F. Miller for his many helpful discussions on epitaxy.

I am most grateful to Dr. W. H. Gauvin, Dr. W. C. Cooper, and Canadian Copper Refiners Ltd., for their financial support and provision of materials.

## Contents

	Page
Acknowledgements.	2
Abstract.	6
<u>Chapter 1. Introduction.</u>	7
1.1. Selenium.	7
1.2. The structure of hexagonal selenium.	11
1.3. Previous work.	13
 <u>Chapter 2. Epitaxy.</u>	 23
2.1. Early results.	23
2.2. Theories of epitaxy.	25
2.3. Epitaxial growth of metals.	30
(a) Growth on non metals.	
(b) Growth on metals.	
2.4. Epitaxial growth of non metallic elements.	35
 <u>Chapter 3. Experimental arrangements.</u>	 39
3.1. Introduction.	39
3.2. The vapour source.	39
(a) The charge support.	
(b) The selenium charge.	
3.3. Choice of substrates.	42
3.4. Preparation of the substrate surface.	44
(a) Cleaved sodium chloride (rock salt) and potassium bromide.	
(b) Polished rock salt and potassium bromide.	



- (c) Cleaved calcium fluoride, barium fluoride and magnesium oxide.

3.5. The deposition of films. 51

- (a) The vacuum system.
- (b) The evaporation chamber.
- (c) Measurement of substrate temperature.
- (d) Evaporation procedure.

3.6. Removal of films from substrates. 61

- (a) Removal from alkali halides.
- (b) Removal from barium fluoride, calcium fluoride and magnesium oxide.

Chapter 4. Electron diffraction and micrography of films. 65

4.1. Introduction. 65

4.2. Selenium films on sodium chloride (rock salt). 68

- (a) Cleaved (100) sodium chloride.
- (b) Polished (110) sodium chloride.
- (c) Polished (111) sodium chloride.
- (d) The diffraction pattern given by selenium on (100), (110), and (111) sodium chloride.

4.3. Selenium films on (100) potassium bromide. 73

- (a) Analysis of diffraction pattern.
- (b) Orientation of selenium on the substrate.
- (c) Influence of substrate temperature.
- (d) Influence of film thickness on orientation.

(e)	Influence of deposition rate.	
(f)	Selenium deposited on polished (100) potassium bromide.	
4.4.	Selenium films on polished (110) potassium bromide.	94
(a)	Analysis of the diffraction pattern.	
(b)	Orientation of selenium on the substrate.	
4.5.	Selenium films on polished (111). potassium bromide.	104
4.6.	Selenium films on (111) calcium fluoride.	104
4.7.	Selenium films on (111) barium fluoride.	105
4.8.	Selenium films on (100) magnesium oxide.	105
<u>Chapter 5.</u>	<u>Determination of film thickness.</u>	112
5.1.	Introduction.	112
5.2.	Fluorimetric determination of selenium.	113
<u>Chapter 6.</u>	<u>Discussion of results and Future work.</u>	116
6.1.	Discussion of results.	116
6.2.	Future work.	119

## Abstract

Thin films of selenium have been prepared on single crystal substrates by vacuum evaporation of selenium and condensation onto the heated substrate.

Reviews are given of the phenomenon of epitaxy, the structure of the allotropes of selenium, and the previous work on selenium films having any bearing on the problem of epitaxial growth.

Techniques are described for the preparation of single crystal substrates, the deposition of selenium films, and their removal from the substrate. Transmission electron micrography and diffraction were used to examine the films. Conditions were established for the epitaxial growth of selenium on (100) and (110) potassium bromide, and the relative orientations of the film and the substrate determined. Films were also prepared on (100), (110), and (111) sodium chloride, (111) potassium bromide, (100) magnesium oxide, and (111) calcium and barium fluoride. These latter films were found to be polycrystalline or amorphous. Film thickness was determined by the measurement of the area and the chemical determination of the mass of the film.

The structure and orientation of the films is discussed in terms of misfit of the substrate and overgrowth lattices, and particularly in terms of recent work on crystal surfaces.



## CHAPTER I - Introduction

### 1.1. Selenium - general

Selenium is one of the members of group VIb of the periodic table which form long chain structures; the others are sulphur and tellurium.

Selenium was discovered in 1817 by J.J. Berzelius<sup>1</sup> as part of the deposit found on the floor of a sulphuric acid plant after the roasting of pyrites. He subsequently examined the properties of the element in detail. The ionic radii of sulphur ( $S^{2-}$  1.74Å) and selenium ( $Se^{2-}$  1.91Å) are close enough for many sulphides and selenides to be isomorphous. The average ratio of selenium to sulphur in sulphur ores is approximately 1:6000<sup>2</sup>.

The main source of selenium is as a biproduct of the recovery of non ferrous metals from their sulphides. Tellurium is another biproduct of this process. No commercially exploitable ores of these elements have yet been discovered.

Selenium exists in a number of allotropic forms, as shown in Table 1.



TABLE 1

Allotropic form	Molecular form	M.P.	B.P.
gas	Varies from $\text{Se}_8$ and $\text{Se}_6$ at $500^\circ\text{C}$ to $\text{Se}_2$ at about $1400^\circ\text{C}$ . Some evidence of dissociation $\text{Se}_2 \longrightarrow 2\text{Se}$ at $2000^\circ\text{C}$ <sup>5,6.</sup>		
Liquid	Equilibrium mixture of long chains and $\text{Se}_8$ or possibly $\text{Se}_6$ depending upon temperature. Average chain length approx. 500 atoms.		$688^\circ\text{C}$
Vitreous Amorphous	Supercooled liquid <sup>7,8,9,10.</sup> Similar to liquid	35 to $40^\circ\text{C}$	
Monoclinic $\alpha$ and $\beta$	$\text{Se}_8$ rings <sup>11,12,13,14,15</sup> $\alpha$ and $\beta$ monoclinic appear to be identical <sup>14.</sup>		
Hexagonal	Parallel long chains held together by Van der Waals forces <sup>16,17,18.</sup>	$217^\circ\text{C}$	
Cubic $\alpha$ and $\beta$	Both forms only recently discovered with only electron diffraction evidence. Possibly due to splitting of chains by the electron beam <sup>19,20.</sup>		

The only stable form of selenium from room temperature to 217°C appears to be the hexagonal phase, all other forms being metastable and transforming to this at a rate dependent upon temperature.  $\Delta H$  for the transformation amorphous  $\longrightarrow$  hexagonal is 15 Cal/gm<sup>21</sup>, and monoclinic  $\longrightarrow$  hexagonal 2.2 Cal/gm<sup>22</sup>. The two cubic forms were discovered by Andrievskii<sup>19</sup> in 1959, on the evidence of electron diffraction data. Very little data is available on their stability, but this structure would be expected to be less stable than the hexagonal.

Due to the fact that selenium is photosensitive<sup>3</sup>, and the electrical resistance of a hexagonal selenium to metal junction is dependent upon applied voltage<sup>4</sup>, the physical properties of selenium have been widely studied. This has led to the development of the photocell, the metal rectifier and new photo recording materials. Because of this however, most of the investigations have been concerned with microcrystalline selenium (an ill defined mixture of amorphous and hexagonal crystalline material), or amorphous selenium. The electrical properties of microcrystalline selenium are very sensitive to structure and impurity levels<sup>23</sup>. Any factor which causes breakage of the polymer chains modifies the crystallization and the electrical properties. The factors controlling crystallization are temperature and

and impurity levels. Hedman<sup>24</sup> has in fact shown the profound effect on nucleation of a few parts per million of oxygen in amorphous selenium. For the above reasons the work on microcrystalline material has done little to broaden the knowledge of the basic physical properties of selenium.

Single crystals of hexagonal selenium have been grown and studied, notably by Henkels(1951)<sup>25</sup> who grew crystals from a melt, and Flessner(1951)<sup>26</sup> who grew them from the vapour. It has been suggested that difficulties in interpretation of the electrical data from these crystals could arise from two sources.

(a) That selenium is an extrinsic semiconductor, and anomalies are due to the effect of impurities<sup>26</sup>.

(b) That the effects are due to potential barriers in the structures of selenium itself. The barriers occur where the charge carriers move from one chain to another<sup>27,28</sup>.

It would seem desirable that any further work on selenium should be carried out under complete cleanliness, and in a way which allows examination of structural details. This type of investigation has been carried out with other elements in the form of epitaxial films grown in vacuum<sup>29</sup>. It enables single crystals to be grown, and measurements taken under high vacuum. The examination



of the structure of the sample is then performed in the electron microscope.

For such a technique to be applied to selenium it is first necessary to determine the conditions favourable to the growth of oriented selenium films. The work in this thesis was therefore aimed at investigating the structure of selenium evaporated onto single crystal ionic substrates.

### 1.2. Structure of Hexagonal Selenium

Using X Ray diffraction the structure of hexagonal selenium was investigated by Bradley<sup>30</sup>, Slattery<sup>31</sup>, Straumanis<sup>32</sup>, and Bernal<sup>33</sup>. It was found that there were no discrete selenium molecules, but an aggregate of screw like long chains arranged spirally about the C axis, the C axes of the chains being parallel. Each selenium atom has two nearest neighbours in the same chain, and four next nearest in adjacent chains. The lattice constants determined by Straumanis are  $a = 4.3552\text{\AA}$ , and  $c = 4.9495\text{\AA}$ . (see Fig.1.)

Atoms are bound to their two nearest neighbours by covalent bonds with a bond angle of  $105^\circ$ . Bonding between the chains is of the Van der Waals-London polarization type. Von Hippel(1948)<sup>34</sup> in a theory based on Pauling's(1940)<sup>35</sup> theory of quantum mechanical resonance, proposed hexagonal selenium as a resonance structure,



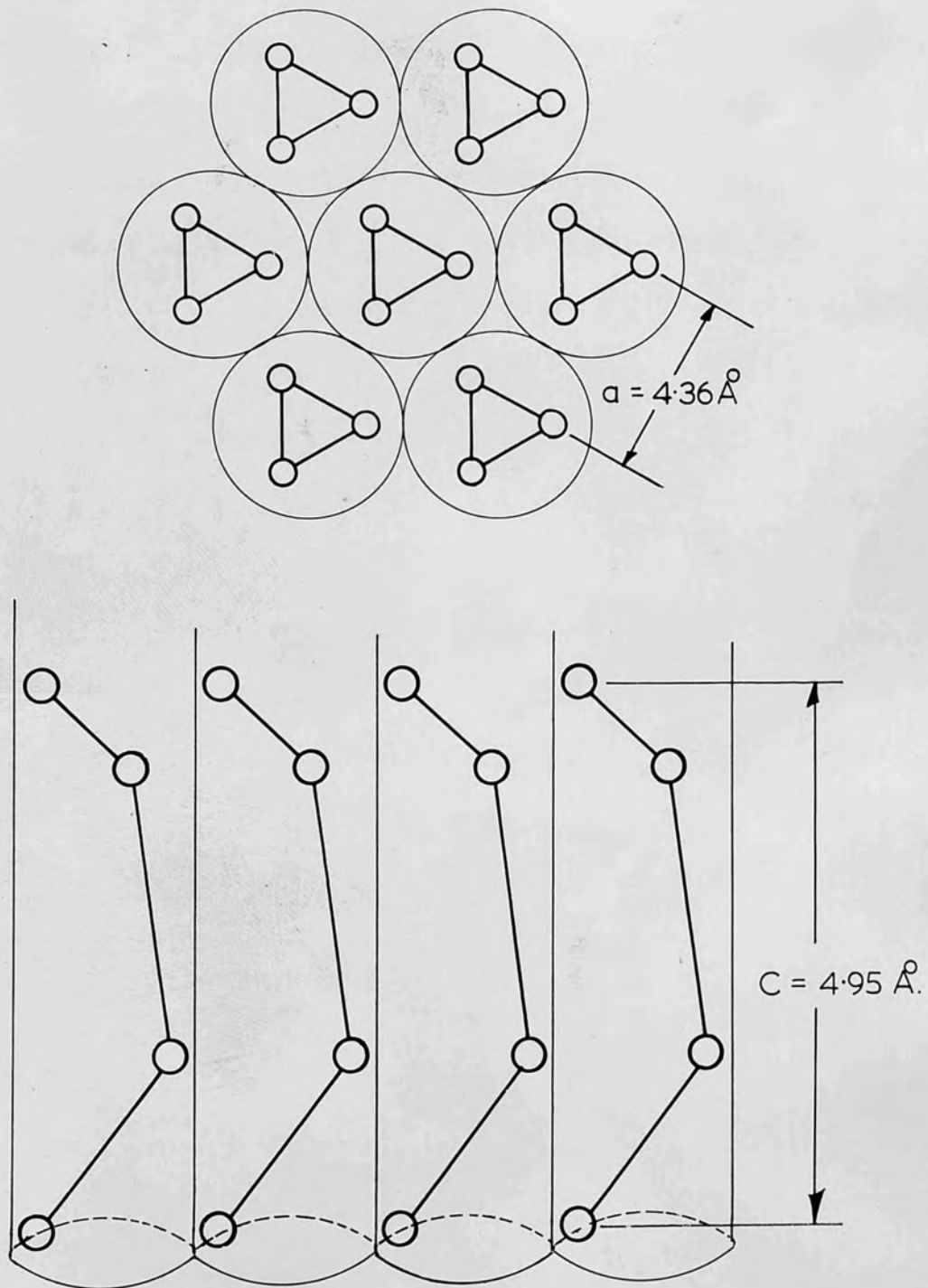


FIG. I. CRYSTAL STRUCTURE OF HEXAGONAL SELENIUM.

the two contributing structures being the insulating hexagonal structure, and a conducting metallic type simple cubic structure. This theory was based on the ease with which the selenium hexagonal lattice could be deformed into a cubic lattice, and the supposedly abnormal Van der Waals radius ( $3.49\text{\AA}$ ). The Van der Waals radius in thallos-thallic selenide is  $3.84\text{\AA}$ . However Hyman (1955)<sup>27</sup> pointed out that the latter compound is considerably ionic, and the selenium atoms negatively charged. Also selenium shows none of the characteristics of metallic bonding. The bonding between the chains is therefore taken as purely Van der Waals type.

The unit cell contains three atoms which are in special positions of one or other of the enantiomorphic space groups  $D_3^4$  or  $D_3^6$

$$D_3^4 : u00; \bar{u}\bar{u}\bar{u}; 0u\bar{u}.$$

$$D_3^6 : u00; \bar{u}\bar{u}\bar{u}; 0u\bar{u}.$$

where  $u$  is  $.217$  (Wyckoff 1948).

These values make the length of the Se - Se bond along the chains  $2.32\text{\AA}$ .

### 1.3. Previous Work

Interest in the structure and properties of evaporated selenium films has been mainly due to the electrical and optical properties of the element. Commercially,

photovoltaic cells of microcrystalline hexagonal selenium are important. However in recent years interest has centred on the amorphous form, and its photoconductivity. Consequently in most of the work selenium has been evaporated onto transparent amorphous, or polycrystalline substrates.

Measurements of absorption spectrum and absorption coefficient have been made by Gilleo(1951)<sup>36</sup>, Dowd(1951)<sup>37</sup>, Stuke(1953)<sup>38</sup> and Hilsum(1956)<sup>39</sup>. Gilleo(1951), Stuke(1953) and Stegman(1957)<sup>40</sup>, also studied the change in absorption spectrum on converting the amorphous film to a microcrystalline hexagonal film. However, these workers evaporated selenium onto cold glass substrates to give an amorphous layer, and then crystallized this by heat treatment. Photoconductivity measurements on evaporated films have been made by Moss(1952)<sup>41</sup>, Gilleo(1951)<sup>36</sup>, Weiner and Cope(1951)<sup>42</sup>, and Potland(1960)<sup>43</sup>. Again however these were amorphous films, and where hexagonal films were used there is no data on their structure.

Richter and Herre(1958)<sup>44</sup>, Andrievskii(1959)<sup>45</sup>, and Semiletov(1960)<sup>20</sup> have evaporated amorphous selenium films onto amorphous substrates, and examined the resulting structure after heat treatment.

Only Semiletov found any appreciable orientation of the deposit, and this is probably due to temperature



gradients during heat treatment, and the presence of thallium in relatively large amounts. He shows an electron diffraction pattern of this film consisting of a series of arcs, with no ring pattern at all. (Fig.2.) The pattern illustrated is claimed to show the basal faces of the crystals parallel with the substrate surface, but the arcs in this pattern show no signs at all of three fold symmetry, and indicate rather orientation of the C axis parallel to the substrate.

Although two workers, Chihaya(1955)<sup>46</sup> and Schossberger (1961)<sup>47</sup> have evaporated selenium onto single crystal substrates neither have reported any signs of epitaxy occurring. Chihaya condensed selenium onto cleaved rock salt surfaces at temperatures from 100°C to 200°C, and compared these with films on formvar similarly prepared. The films on rock salt showed a higher degree of crystallinity but no signs of epitaxy were reported.

Schossberger chose the (100) cleavage plane of magnesium oxide, and condensed selenium onto this at room temperature and 112°C. At room temperature only a small amount of crystalline material was formed, but on annealing the film and substrate at 150°C some preferential orientation of the selenium (1010) plane parallel to the substrate was observed. Increasing the substrate temperature to 112°C during evaporation resulted in only a small amount of



hexagonal selenium together with an unknown phase. The author of this paper infers that the degree of orientation observed on magnesium oxide will be typical of selenium on any single crystal substrate. This reasoning is however completely unjustified considering the present knowledge of epitaxial growth, and ignores the influence of the substrate lattice and lattice parameters.

The only claimed example of epitaxial growth by selenium found in the literature is that by Hyman(1956)<sup>48</sup>. He evaporated selenium under argon onto a glass substrate at 205°C. The hexagonal crystals formed on this surface took the shape of a central spine, from which grew similar spines or branches. The branches grew at an angle of  $40 \pm 3^\circ$  to the central spine in some cases and  $90^\circ$  in others.

Using the diagram shown in Figure 3, Hyman gives lattice misfits of 14 and 25% respectively for the  $90^\circ$  and  $41^\circ$  directions of secondary needles. The stated misfits are said to be within the permitted limits for epitaxial growth. Limiting values of misfit for the occurrence of epitaxial growth are however no longer accepted as valid (See Chapter 2). No planes of contact between the lattices are specified, but in the case of needles at  $40 \pm 3^\circ$ , they must be the (11 $\bar{2}$ 2) and the prism face (10 $\bar{1}$ 0). This would mean that the two axes were at  $41^\circ$ . Where

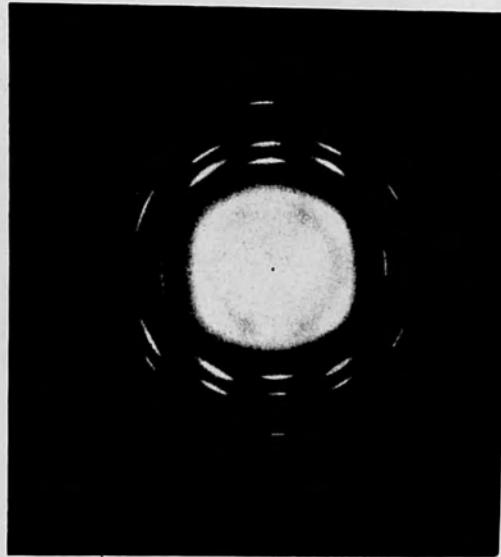
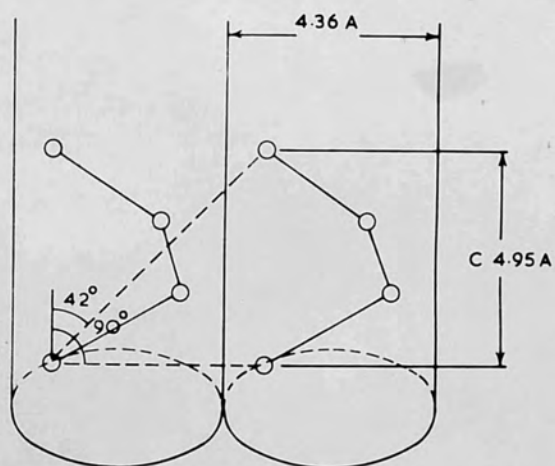


Fig. 2. Electron-diffraction pattern of a film of hexagonal selenium with the basal faces of its crystals parallel to the backing (texture axis [0001]).

FIGURE 2. (Semiletov. 1959.)



THE CRYSTAL STRUCTURE OF HEXAGONAL SELENIUM.

DOTTED LINES SHOW PREFERRED DIRECTIONS OF C-AXIS IN EPITAXIAL GROWTH

FIGURE 3. (Hyman. 1955.)

the needles at  $90^\circ$  are concerned, the basal plane (0001), must be sitting on the prism face (10 $\bar{1}$ 0). Misfit diagrams showing the superposition of these lattice planes are shown in Figures 4 and 5.

No positive evidence of epitaxy is presented in Hyman's paper, and the probability of its occurrence would seem small compared with that of a continuation of the lattice.

The photograph shown in the paper of crystals illustrating the  $90^\circ$  case, also shows that the branch needles terminate in a face at approximately  $45^\circ$  to the C axis. It therefore seems quite possible that some mechanism other than epitaxy is responsible for the growth pattern.

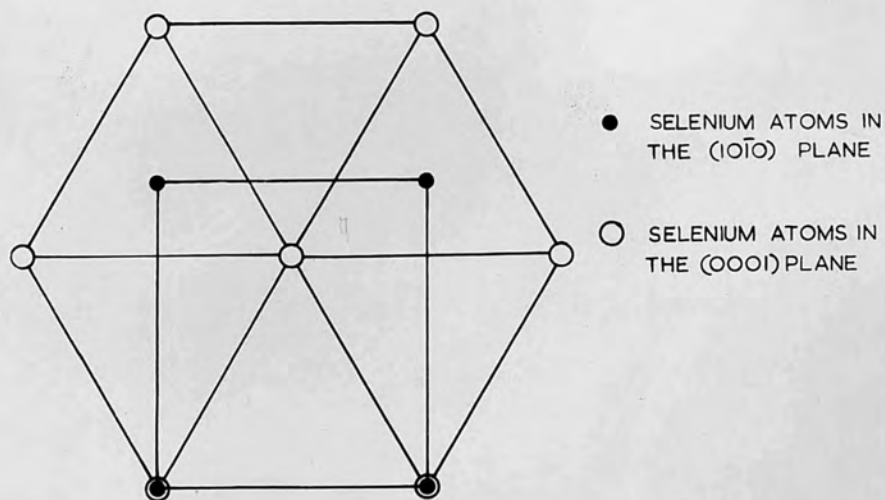


FIG.4. MISFIT DIAGRAM FOR SELENIUM  $(0001)$  PLANE ON THE  $(10\bar{1}0)$  PLANE.

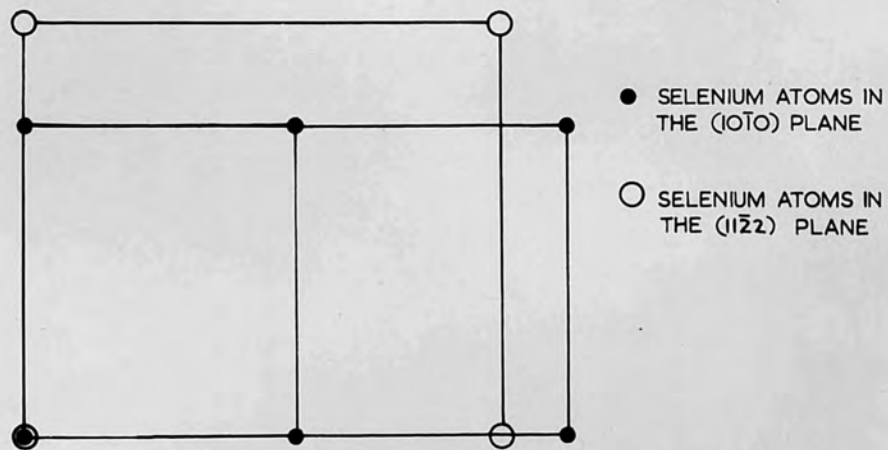


FIG.5. MISFIT DIAGRAM FOR SELENIUM  $(1\bar{1}22)$  PLANE ON THE  $(10\bar{1}0)$  PLANE.



References to Chapter 1.

1. Berzelius, J.J. (1818), Acad. Handl. Stockholm, 39, 13.
2. Goldschmidt, V. (1954), Geochemistry, O.U.P.
3. Smith, W. (1873), Soc. Tele. Eng. Jrl., 2, 31.
4. Adams, W.G. and Day, R.E. (1878). Phil. Mag., (5), 3, 295.
5. St. Deville, H. and Troest, L. (1863),  
Bull. Soc. Chim (1), 5, 434.
6. Freuner, G. and Brockmüller, J. (1913),  
Zeit. Phys. Chem, 81, 129.
7. Krebs, H. and Schultz Gebhardt, F. (1954),  
Naturwiss., 41, 474.
8. McCullough, D. (1936), Ph'd Thesis, Caltec.
9. Richter, H. and Herre, F. (1958),  
Z. Naturforsch., 13A, 874.
10. Richter, H. and Herre, F. (1957), Naturwiss., 44, 31.
11. Warren, B. and Burwell, J. (1935), J. Phys. Chem., 3, 6.
12. Klug, H.P. (1934), Z. Krist., A88, 128.
13. Burbank, R.D. (1952), Acta. Cryst., 5, 236.
14. Marsh, R.E. and Pauling, L. (1953), Acta. Cryst., 6, 71.
15. Halla, F., Bosch, F. and Mehl, E. (1931),  
Z. Physik. Ch., B11, 455.
16. Bradley, A.J. (1924), Phil. Mag., 48, 477.
17. Slattery, M. (1925), Phys. Rev., 25, 333.
18. Straumanis, M. (1940), Z. Krist., 102, 432.
19. Andrievskii, A. et al. (1959), Doklady. Akad. Nauk.  
S.S.S.R., 124(2), 321.
20. Semiletov, S.A. (1960), Soviet Physics Crystallography,  
4, (4), 588.

21. Dorabialka.A. (1957), *Zeszyty. Nauk. Politech. Lodz.Chem.*, 6, 45.
22. Das Gupta.K. and Das.S.R. (1941), *Nature*, 143, 165.
23. Henkels.H.W. (1951), *J.Appl.Phys.*, 22, 10, 1265.
24. Hedman.L.E. (1962), *Arkiv För Fysik*, 21, (13), 161.
25. Henkels.H.W. (1951), *J.Appl.Phys.*, 22, (7), 916.
26. Flessner.K.W. (1951), *Proc.Phys.Soc.B.*, 64, 671.
27. Nyman.R.A. (1955), Ph'd Thesis. Reading Univ.
28. Moss.T.S. (1959), *Optical Properties of Semiconductors*. (Butterworths).
29. Mayer.H. (1959), *Structure and Properties of Thin Films - International Conference 1959*. (John Wiley & Sons. Inc.)
30. See reference 16.
31. See reference 17.
32. See reference 18.
33. Bernal.J.D. (1929), *Trans.Faraday Soc.*, 25, 375.
34. Von Hippel.A. (1948), *J.Phys.Chem.*, 16, 372.
35. Pauling.L. (1940), *Nature of the Chemical Bond*. (Cornell Univ.Press.)
36. Gilleo.M.A. (1951), *J.Chem.Phys.*, 19, 1291.
37. Dowd.J.J. (1951), *Proc.Phys.Soc.Lond.*, B69, 506.
38. Stuke.J. (1953), *Z.Phys.Lpz.*, 134, 194.
39. Hilsum.C.(1956), *Proc.Phys.Soc.Lond.*, B69, 506.
40. Stegman.H. (1957), *Naturwiss.*, 44, 108.
41. Moss.T.S. (1952), *Photoconductivity in the Elements* (Butterworths, London).
42. Weimer.P.K. and Cope.A.D.(1951), *R.C.A.Review*, 12, 314.

43. Fotland.R.A. (1960), J.Appl.Phys. 31, (9), 1558.
44. Richter.H., and Herre.F. (1958), Z.Naturforsch, 13A, 874.
- × 45. Andrievskii.A.I.et al. (1959), Doklady Akad Nauk. *Rvt*  
S.S.S.R., 124 (2), 321.
46. Tadashi Chihaya. (1955), Nippon Kinzoku Gakkaishi., 19,47.
47. Schessberger.F. and Ticulka.F. (1961),  
Trans 8th Nat.Vac.Symp., 2, 1001.  
(American Vacuum Society).
48. Hyman.R.A. (1956), Proc.Phys.Soc., LXIX, 687.
49. Pashley.D.W. (1956), Advances in Physics., 5, 173.



## CHAPTER 2. - Epitaxy

### 2.1. Early Results

The term epitaxy ('arrangementton') was introduced by Royer(1928)<sup>50</sup> to denote the oriented growth of one crystal on another. This was first observed in natural crystals but has led to similar growth being produced in the laboratory by a variety of means. Examples of this are, growth from solution (Frankenheim.1836)<sup>51</sup>, chemical action (Aminoff and Broome.1936)<sup>52</sup>, electrodeposition (Cochrane.1936)<sup>53</sup>, and condensation from the vapour phase (Bruck.1936)<sup>54</sup>. Optical microscopy, X-ray and electron diffraction have been widely used in the study of epitaxial growth, and comprehensive reviews of the results using these methods have been written by Van der Merwe(1949)<sup>55</sup>, Seifert(1953)<sup>56</sup>, and Pashley(1956)<sup>49</sup>. Attempts have been made to form empirical rules governing epitaxial growth. Royer(1928)<sup>50</sup> deduced three rules from observations on growth from solution: these were:-

(a) That oriented growth occurs only when it involves the parallelism of two lattice planes which have networks of identical or quasi-identical form, and of closely similar spacings. This implies a minimisation of the degree of misfit between the parallel lattice spacings. Percentage misfit is defined as

$$\frac{100 (b - a)}{a}$$

where  $a$  and  $b$  are the corresponding lattice spacings in the substrate and overgrowth respectively. Royer's results suggested a maximum possible misfit of 15%.

(b) That where ionic crystals are involved, the ions of the overgrowth should take up positions which corresponding ions of the substrate of the same polarity would have occupied had the substrate continued to grow.

(c) That the substrate and the overgrowth should have the same type of bonding.

Data which has been accumulated since Royer's work has shown that these rules are not necessarily obeyed. There are numerous examples of mutual orientation between ionic and metallic crystals (Bruck 1936), and also covalently bonded selenium on ionic substrates (Chapter 4). Epitaxial deposits on heated rock salt do not generally form in the orientation predicted by rule (a). Collins and Heavens(1957)<sup>57</sup> obtained the orientation  $(100)[100]$  Ni on  $(100)[100]$  NaCl with - 37% misfit rather than  $(100)[100]$  Ni on  $(100)[110]$  NaCl which has the smaller misfit of - 11.5%.

It is evident that the probability of epitaxy occurring in any particular case, and the degree to which it occurs depends strongly on the prevailing conditions. This is illustrated by the results obtained when both substrate and overgrowth are alkali halides. Although Royer(1928) and Sloat and Menzies(1931)<sup>58</sup> found fairly well defined misfit limits (-13% to +9% for a KCl substrate) for growth

from solution, Schultz(1951)<sup>59</sup>, and Ludemann(1954)<sup>60</sup> found no such limits for growth from the vapour phase. Any alkali halide grew epitaxially on any other alkali halide, with the range of misfits (-4% to +90%) limited only by the lattice constants available. Doubt has also been cast recently on the minimum temperatures for epitaxy observed by Bruck(1936) for vapour deposited metals on alkali halides. Sloope and Tiller(1961)<sup>61</sup> found that the "epitaxial temperature" for silver evaporated onto rock salt varies with the rate of deposition.

The influence of cleanliness of the substrate surface on the epitaxial temperature was demonstrated by Trillat and Sella(1963)<sup>62</sup>. They found that the temperature for the perfect parallel orientation of gold on rock salt was lowered from 400°C to 200°C by simultaneous cleavage and film deposition in vacuum.

## 2.2. Theories of Epitaxy

The theoretical treatments of epitaxy have in general been based on the concept of good fitting between the substrate and overgrowth. Frank and Van der Merwe(1949)<sup>63</sup> put forward a theory assuming that the initial stage of growth is an immobile two dimensional monolayer with a regular atomic pattern. This monolayer is homogeneously deformed so as to have the same spacing as the substrate, i.e. to form a pseudomorphic first layer. The conditions



for stability in such a system are examined when it is subjected to a periodic force due to the substrate atoms, assuming the overgrowth to cohere under the action of a linear force law. This system is shown to be unstable for misfits of greater than 9%, with a possible metastable configuration having up to 14% misfit at low temperatures. Once this layer has formed, a macroscopically thick layer can be formed by repetition of the process. Further layers are subjected to successively less strain, until the strain free bulk deposit is obtained. Smollet and Blackman(1951)<sup>64</sup> have criticised the theory on the grounds that it predicts monolayers which would not necessarily be stable. Two dimensional arrays of atoms were considered representing the lattice planes of various alkali halides. Several pairs of alkali halides were considered between which epitaxy is known to occur, and it is shown that for many cases the strain required to produce a monolayer of deposit material to fit the substrate would lead to instability. Conversely in certain cases where a strained monolayer would be stable epitaxy does not occur. It was therefore concluded that the orientation observed experimentally did not arise from a pseudomorphic layer. Evidence for and against the presence of a strained monolayer is conflicting. The term "basal plane pseudomorphism" was introduced by Finch and Quarrel(1933)<sup>65</sup> in an

attempt to explain the results obtained for the growth of ZnO on Zn.

Certain electron reflection diffraction rings were interpreted as a modified oxide structure caused by the constraining influence of the zinc substrate. Other observations of modified spacings were also interpreted as the effects of pseudomorphic growth by Cochrane(1936)<sup>53</sup>, Miyake(1938)<sup>66</sup>, and Clark, Fish, and Weeg(1944)<sup>67</sup>.

Pashley(1956)<sup>49</sup> has re-examined these results in the light of more recent work, (Raether 1950<sup>68</sup>, Lucas 1951<sup>69</sup>, Newman 1956<sup>70</sup>), and has shown that in fact there is no justification for their interpretation as proof for pseudomorphism as a mechanism in epitaxy. However Shishakov (1952, 1957)<sup>71</sup> has reported Pt in thin layers with a lattice constant 1.5% greater than that of the bulk material, and Fe with a lattice constant 5% greater than normal in the initial stages of deposition on mica.

The electron diffraction evidence concerning the growth of films during the first few Angstroms indicates that the formation of a monolayer is the exception rather than the rule (Schulz 1952)<sup>72</sup> (Newman and Pashley 1955)<sup>73</sup>.

Films deposited under controlled conditions of vacuum evaporation show that nucleation followed by the formation of three dimensional crystallites occurs (Bassett 1958)<sup>83</sup>. Similar results were obtained for growth from solution

(Newman and Pashley 1955)<sup>73</sup>, and by chemical action (Lisgarten 1954)<sup>74</sup>. In such cases the Frank and Van der Merwe theory does not hold, since it is based on an initial mechanism which is not applicable.

Menzer (1958)<sup>75</sup> suggested that large misfits could be accommodated by the development of twinning in overgrowth layers close to the substrate surface. This was based on data which showed that silver and nickel films grown by vacuum evaporation (Bruck 1936)<sup>54</sup> on rock salt were twinned on their (111) planes at several hundred Ångstroms thickness.

Since the twinned lattices have their (221) planes parallel to the (001) rock salt surface it was suggested by Menzer that the initial nuclei grew with their (221) planes parallel to the rock salt. The misfit for this is less than for the (001) planes. However electron diffraction investigations of the initial stages of growth of metals on rock salt have since thrown doubt on this. Kehoe (Pashley 1956)<sup>49</sup> observed no twinning of silver on rock salt below 10 Ångstroms thickness, and Collins and Heavens (1957)<sup>57</sup> observed no twinning in nickel on rock salt at 20 Ångstroms thickness.

The problem of stability of thin layers has been examined by Drabble (1949)<sup>76</sup> in terms of the co-ordination conditions of the deposited atoms, and it is shown that the observed orientation is frequently governed by a tendency



to continue the substrate structure across the boundary. This preservation of the normal co-ordination of the atoms at the interface is in accordance with Royers second rule. Some evidence in support of this was found by Collins and Heavens (1957)<sup>57</sup>.

The growth of metal deposits on rock salt was considered by Engel (1952)<sup>77</sup> in the light of the assumption that the metal is ionized, and substrate-metal binding forces were largely electrostatic. If the appropriate ionization state of the metal is assumed, then Bruck's epitaxial temperatures are found to increase linearly with ionization potential. The correct orientation is predicted for silver on rock salt, assuming that a monolayer of deposit-metal salt exists at the interface. Later observations of epitaxial temperatures considerably lower than Bruck's by Kehoe (Pashley 1956) and Sloope and Tiller (1961)<sup>61</sup> have however rendered this theory unacceptable.

The chief reason for the failure of existing theories to fit the facts of epitaxy appears to be that they are based on unsuitable models for the growth of initial nuclei. The work of Germer, MacRae and Hartman (1961)<sup>78</sup> shows the role played by adsorbed gases in the structure of Ni films. Trillat and Sella (1963)<sup>62</sup> have examined

the effect of substrate cleanliness on epitaxy and have found it extremely important. Simultaneous cleaving and film deposition in vacuo results in a lowering of epitaxial temperatures, a change in the pattern of crystallite growth, and the occurrence of epitaxy not observed before, when compared with cleavage in air. It seems reasonable to expect adsorbed impurity atoms, mostly gaseous, to take up preferred positions on the substrate surface (Ehrlich 1959)<sup>79</sup>, and greatly modify its properties. Any theory which attempts to explain epitaxial growth on relatively dirty surfaces (conditions under which epitaxy has largely been studied) will therefore fail if it does not take into account the role of adsorbed impurities.

It appears that before the problems can be solved more knowledge of initial nucleation, and the surface forces involved in this, will be required.

### 2.3. Epitaxial growth of metals.

The epitaxial growth of metals on single crystal substrates has been studied largely by vacuum evaporation, and examination of the resultant film by electron diffraction and microscopy. Although some of the early work was done on electrolytically deposited films, vacuum evaporation is far cleaner, and more easily controlled.

(a) Growth on non metals.

The most popular substrate for the growth of metals has been the cleavage face of rock salt. Metal vapours condensed on cold rock salt give either a randomly oriented polycrystalline film, or a some degree of textured orientation depending on the angle of incidence of the vapour beam.

On the other hand condensation onto rock salt heated to a suitable temperature often leads to the formation of a highly oriented layer consisting of large crystals. This acquires the structure of a mosaic single crystal accurately oriented with respect to the rock salt crystal. This also holds true for the deposition of metal vapours on many other single crystal substrates.

Bruck (1936)<sup>54</sup> investigated the orientations of films of Au, Ag, Al, Cu, Ni, Fe, Co, Cr, and Pd, deposited on heated rock salt from the vapour. A minimum epitaxial temperature was found for each. This is however dependant on deposition conditions (Trillat and Sella 1963)<sup>62</sup>. It was also found from transmission electron diffraction of the detached films that,

1. Orientation apparently improved with thickness.
2. Irrational reflections were present in the



diffraction patterns. These have since been shown to be mainly caused by repeated twinning on the (111) type planes (Menzel 1958<sup>75</sup>, Reimer 1959<sup>80</sup>, Burbank and Heidenreich 1960<sup>81</sup>).

3. Differences exist between the orientation of the face centred cubic metals and the body centred cubic metals, the former being oriented with their (100) planes parallel to the cube face of rock salt, and their cube edges parallel with the cube edges of the rock salt, while the latter have their cube edges parallel to the diagonal across the rock salt face. Other orientations of the body centred cubic metals may exist at different temperatures (Shirai - See Pinsker 1953)<sup>82</sup>.

Growth of metals on polycrystalline substrates, even at high temperatures produces only polycrystalline films with no regular azimuthal orientation.

From the work of Bassett (1958)<sup>83</sup> and others (Bassett and Pashley 1959)<sup>84</sup> it is obvious that three dimensional nuclei are first formed when a metallic vapour is condensed on rock salt. Electron micrographs of gold nuclei of  $10^8$  size show that nucleation takes place preferentially along cleavage steps in the rock salt surface, the distribution in between being random.

Further deposition results in an increase in crystallite size until the substrate surface is completely covered at a thickness of  $1000\text{\AA}$ . A high density of crystal faults are observed, in the order of  $10^{11}$  dislocations per  $\text{cm}^2$ .

Pashley has made a cine-film of gold growing epitaxially on molybdenum disulphide. The film shows an initial distribution of three dimensional nuclei, some growing at the expense of others, until a mosaic of oriented crystallites is formed with empty channels in between.

The crystallites are shown to be crystallographically ordered, yet the transfer of atoms from one nucleus to another appears to be possible, the larger of two neighbouring nuclei increasing in size while the other diminishes. Channels between the crystallites are also filled in by a process similar to the joining of liquid drops, inspite of the fact that the main bulk of each gives rise to typical crystalline diffraction contrast features. Although films grown under such conditions are subject to electron bombardment, and the usual contamination of cracked pump oil, and residual gases, a high degree of mobility of the initial nuclei is indicated. The relationship between the arriving deposit atoms and the substrate

appears to be a dynamic one likely to involve complex surface forces.

(b) Growth on metals.

The first investigations of metal films on metal single crystal substrates were those on electrolytic deposits. Cochrane (1936)<sup>53</sup> used etched (111) and (110) faces of single crystal copper as substrates for the electrodeposition of Ni, Cu, Zn, Cd, Ag, Cr, and Co. Electron diffraction showed that there was an upper limit of current density for the production of oriented deposits of the face centred cubic metals. Irrational reflections observed were associated with twinning, and Zn and Cd showed no orientation. Bruck (1936)<sup>54</sup> examined the mutual orientation of Au and Ag by epitaxial growth of the substrate metal on rock salt first. Oriented growth occurred above a minimum temperature. Bassett and Pashley (1959)<sup>84</sup> have examined the initial stages of the growth of gold on thick single crystal films of silver on mica, and found the mode of growth to differ from gold on rock salt. Three dimensional nuclei are still formed but the gold spreads more easily over the silver surface and forms a continuous layer at about 100Å thicknesses. This is probably due to the difference between the substrate-deposit binding forces and the smaller misfit of gold on silver.



The latter effect of better spreading for lower misfit has been observed by Schulz for the growth of alkali halides on one another - see Gomer and Smith (1953).

#### 2.4. Epitaxial growth of non metallic elements.

The study of the epitaxial growth of non metallic elements has become of interest only in recent years, and has been due mainly to the new importance of silicon and germanium as semiconductors. Both have been grown epitaxially on themselves and on other single crystal substrates. Germanium was epitaxed on its own (100), (110) and (111) faces by Weinreich, Dermit, and Tufts (1961)<sup>86</sup>, Semiletov (1956)<sup>87</sup>, and Kurov et al (1957)<sup>88</sup>. There is some disagreement amongst these workers concerning epitaxial temperatures, presumably due to different degrees of substrate contamination.

Collins and Heavens (1952)<sup>89</sup> epitaxed germanium onto heated rock salt, and also on epitaxially grown silver. Both germanium and silicon have been epitaxed onto (111) calcium fluoride by Via and Thun (1961)<sup>90</sup> good oriented growth occurring only at low evaporation rates.

No study of epitaxial growth mechanisms comparable with those on metals have been carried out with non metals but it is presumed that the growth mechanisms are similar.

## REFERENCES TO CHAPTER 2.

50. Royer L. (1928), Bull. Soc. Franc. Min., 51, 7.
51. Frankenheim M.L. (1836), Ann.Phys., 37, 516.
52. Aminoff G. and Broome B. (1936), Nature, Lond., 137, 995.
53. Cochrane W. (1936), Proc.Phys.Soc., 48, 723.
54. Bruck L. (1936), Ann.Phys., 26, 233.
55. Vander Merwe J.H. (1949), Disc. Faraday Soc., 5, 201.
56. Seifert H. (1953), Structure and Properties of Solid Surfaces (Chicago Univ. Press).
57. Collins L.E. and Heavens O.S. (1957), Proc.Phys.Soc.,  
B 70, 165.
58. Sleat A.C. and Menzies A. (1931), J.Phys.Chem., 35, 2005.
59. Schulz L.G. (1951), Acta Cryst., 4, 483.
60. Laudemann H. (1954), Z.Natureforsch., 8A, 252.
61. Sloope B. and Tiller C. (1961), J.Appl.Phys., 32, 1331.
62. Trillat J. and Sella C. (1963), Conference on Single Crystal Films 1963 Blue Bell, Pennsylvania, U.S.A.
63. Frank F.C. and Vander Merwe J.H. (1949),  
Proc.Roy.Soc., A 198, 216.
64. Smollet M. and Blackman M. (1951), Proc.Phys.Soc.,  
A 64, 683.
65. Finch G.I. and Quarrell A.G. (1933), Proc.Roy.Soc.,  
A141, 398.
66. Miyake S. (1938), Sci.Pap.Inst.Phys.Chem.Res.Japan,  
34, 565.
67. Clarke G.L., Fish G., Weeg, L.E. (1944), J.Appl.Phys.,  
15, 193.
68. Raether H. (1950), J.Phys.Radium., 11, 11.

69. Lucas L. (1951), Proc. Phys.Soc., A64, 943.
70. Newman R.C. (1956), Proc.Phys.Soc., B69, 432.
71. Shishakov N.A. (1952), Zh.Eksper. Teor.Fiz.,  
22, 241.
72. Schulz L.G. (1952), Acta Crysts, 2, 130.
73. Newman R.C., and Pashley D.W. (1955), Phil.Mag.,  
46, 927.
74. Lisgarten N.D. (1954) Trans. Faraday Soc.,  
50, 684.
75. Menzer G. (1938), Naturwiss., 26, 385.  
and Z.Krist, 99, 385.
76. Drabble J. (1949), Ph'd Thesis. University of  
London.
77. Engel O.G. (1952), J.Chem.Phys., 20, 1174.
78. Germer L.H., MacRae A.V., Hartman C.D. (1961),  
J.Appl.Phys., 32, 2432.
79. Ehrlich G. (1959), Structure and Properties of  
Thin Films (Intern.Conference 1959)  
John Wiley & Sons.
80. Reimer L. (1959), Optik, 16, 30.
81. Burbank R., and Heidenreich R. (1960), Phil.Mag.  
26, 233.
82. Pinsker Z.G. (1953), Electron Diffraction.  
Butterworths, London.
83. Bassett G. (1958), Phil.Mag. 3, 1042.
84. Bassett G., and Pashley D.W. (1959), J.Inst.,  
Metals, 87, 449.
85. Gomer R., and Smith C.R. (1953). Structure and  
Properties of Solid Surface (Chicago  
Univ.Press).



86. Weinreich O., Dermit G., and Tufts C. (1961)  
J.Appl.Phys., 32, 1170.
87. Semiletov S.A. (1956), Kristallografiya,  
1, 542.
88. Kurov G.A., Semiletov S.A., and Pinsker Z.G.(1957)  
Soviet Phys., Crystallography, 2, 53.
89. Collins L.E., and Heavens O.S. (1952), Proc.Phys.,  
Soc., B65, 825.
90. Via G.G. and Thun R.E. (1961), Transactions of the  
8th. National Vacuum Symposium.  
(American Vac.Soc.) Pergason Press.

## Chapter 3. Experimental Arrangements.

### 3.1. Introduction.

The study of oriented growth on single crystal substrates is most easily done in the electron microscope. The microscope available was a Vickers E.M.5 which is designed basically as an instrument for transmission work, and is rather more difficult to use in reflection. This meant that the selenium overgrowth would have to be thin enough to be at least partially electron transparent, and also fairly easily removed from the substrate.

Vacuum evaporation of selenium and subsequent condensation onto the substrate provides a fairly easily controlled method of preparing such films, and also allows the substrate temperature to be varied. Substrates from which selenium could be removed were chosen, and the preparation of their surfaces investigated in the light of previous work on epitaxy.

### 3.2. The Vapour Sources.

#### (a) The Selenium charge support.

In order to produce the vapour stream of selenium necessary for condensation onto the substrate some form of support for the selenium was necessary. The three forms of support suggested by Holland (1956)<sup>91</sup> for selenium are:-

- (a) A resistance heated conical wire basket.
- (b) A resistance heated metal foil boat.
- (c) A ceramic crucible.

Supports of types (a) and (b) have the advantage of heating the charge directly, and therefore making the evaporation rate quickly and easily controllable. However all metals suitable for the fabrication of these supports are chemically reactive with molten selenium, and are therefore likely to contaminate the charge. Glazed Ceramic crucibles have on the other hand been subjected to prolonged contact with molten selenium without any contamination of the charge being spectrographically detectable.

The crucible chosen for the evaporation of selenium was a "micro combustion boat" of glazed porcelain produced by the Royal Worcester Porcelain Co. These boats have external dimensions 28 x 4 x 4 m.m. and internal dimensions 26 x 2.5 x 3 m.m. The evaporation boat was supported by a piece of shaped tungsten sheet, five thousandths of an inch thick, which also acted as the heating element. This was cut and shaped so that it followed the external wall contours of the evaporation boat, with two lugs left at either end for connection with the rigidly mounted L.T. current supply. (Fig.6).



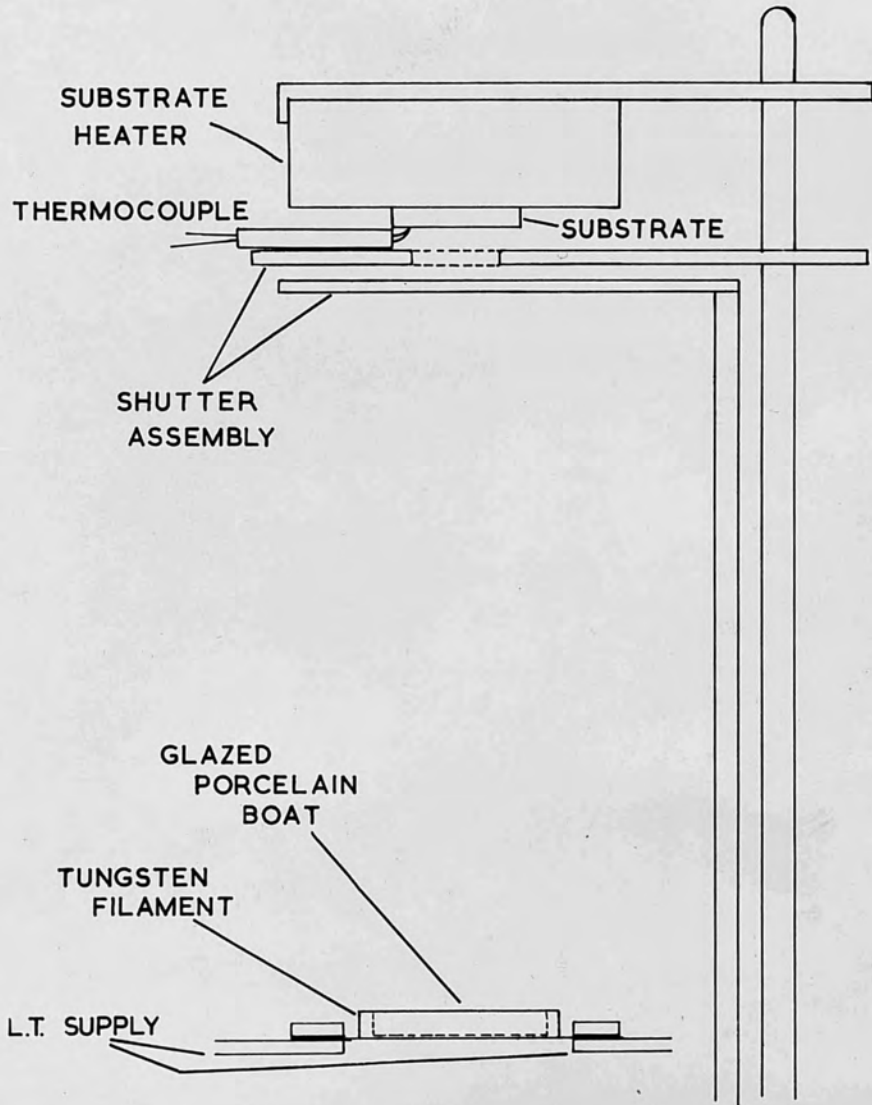


DIAGRAM OF SELENIUM EVAPORATION APPARATUS  
FIG. 6.

(b) The Selenium charge.

The selenium charge for the evaporation boat was supplied by Canadian Copper Refiners Ltd., of Montreal, Canada, in the form of high purity shot of approximately 3 m.m. diameter. Spectrographic and chemical analysis of this material by the producers showed the impurities present to be Te 0.7 p.p.m., Cu 0.04 p.p.m., and Cl 5 p.p.m. No other impurities were detected spectrographically.

The 0.4 gram charge of selenium was melted in the boat and degassed by holding under vacuum at temperature just below the boiling point. When the selenium had stopped bubbling and the chamber pressure had returned to a minimum value the selenium was assumed to be practically free from absorbed gases and ready for evaporation.

3.3. Choice of substrates.

The crystal structures of thin films are appreciably influenced by the type of surface on which they are deposited. Ideally therefore a substrate for epitaxial thin film growth should satisfy the following conditions:-

(a) Atomic flatness and smoothness over the area on which the film is deposited. Micro scale surface irregularities will reveal crystal facets other than those required giving rise to a non uniform lattice

pattern over the surface.

(b) Absolute cleanliness of the surface so that there is no competition between deposit atoms and impurity atoms or molecules for sites on the substrate surface.

(c) No chemical reaction or alloying with the deposit.

(d) A sufficiently low vapour pressure not to interfere with film growth at the required substrate temperature.

(e) A force law between substrate and deposit which favours the formation of an oriented crystalline overgrowth, which if possible is continuous at low thickness.

(f) In this case where the film growth was to be examined in the transmission electron microscope it was also required that the film should be detachable from the substrate.

These requirements are rarely if ever met simultaneously in practice, and the types of substrate required for the satisfaction of condition (e) were unknown. It was decided therefore to investigate initially the structure of selenium films grown on rock salt. This substrate had been widely used in studies of epitaxy and much practical knowledge of preparation technique accumulated. The cleaved (100) face of rock salt had previously been used as a substrate by Chihaya (1955)<sup>46</sup> for selenium with no sign of the



occurrence of epitaxy. Nevertheless it was thought advisable to repeat this work, and also to investigate the structure of selenium evaporated onto the polished (110) and (111) faces. Although epitaxy was not observed on rock salt it was noted that the prism plane of the selenium tended to orient parallel to the rock salt (100) plane.

Assuming the prism face of the hexagonal selenium parallel to the substrate surface, potassium bromide suggested itself as an alternative substrate.

The misfit of the selenium prism plane on the (100) potassium bromide face is only 5% when the C axis is oriented parallel to the [110] direction in the substrate surface, compared with 8.5% for the equivalent orientation on rock salt. Having then observed epitaxial growth on the (100) face of potassium bromide it followed that the degree of orientation on the (110) and (111) faces should also be investigated.

The (111) cleavage faces of calcium and barium fluoride, and the (100) cleavage face of magnesium oxide were also investigated as substrates for epitaxial growth.

#### 3.4. Preparation of the substrate surface.

(a) Cleaved sodium chloride (rock salt) and potassium bromide.

The rock salt and potassium bromide were purchased as artificially grown  $\frac{1}{2}$ " cubes. Both cleave very easily in the (100) plane, but the cleavage faces are crossed by numerous steps. The quality of the crystals received varied considerably, some cleaving easily and giving flat cleavage faces, and others cleaving with some difficulty and showing a great deal of strain.

Crystals to be used as substrates were cleaved in a spring loaded "guillotine", with aligning clamps for the crystal, and stops to prevent the guillotine blade from penetrating more than a millimeter into the crystal.

Cleaved slices about 3 m.m. thick were prepared in this way and immediately placed in the vacuum chamber to minimize atmospheric etching and contamination. A typical example of such a crystal was silvered and examined by means of multiple beam Fizeau fringes (Tolansky 1948)<sup>92</sup>. Figure 7 shows an interferogram of this surface revealing small flat areas terminated by cleavage steps several thousand angstrom units in height.

(b) Polished rock salt and potassium bromide.

In order to obtain sufficiently large (110) and (111) faces on the two alkali halides it was necessary to cut and polish them. For comparison the cleaved (100) faces were also ground and polished.

on solenoidal filter paper was used, and likely to hinder

The (110) and (111) faces had to be cut from the  $\frac{1}{2}$ " cubes. This was done with a reciprocating linen thread band saw, lubricated with water, and driven by a simple arrangement of cranks and pulleys. Correct positioning of the saw cut was ensured by mounting the crystals in specially designed jigs (Figure 8). A brass block with a rectangular U cross section was milled with a plane face *F* intersecting the channel, in such a way as to be parallel to the (110) plane of the alkali halide (within  $\frac{1}{2}$  degree). The crystal was clamped to the bottom and one side of the channel. A similar jig was made for cutting (111) planes. The alkali halide cube projected so that the band saw passing across the face *F*, cut a (110) or (111) type of plane face on the crystal.

When the required face had been cut, the surface was ground completely flat on a water moistened filter paper on a glass plate. The crystal was then moved forward in the jig and a further saw cut made to produce a slab about 3 .m.m. thick. To improve thermal contact between the crystal and the substrate heater during evaporation, the back face of the crystal was also ground flat.

Since the polish produced on the crystals ground on moistened filter paper was poor, and likely to hinder



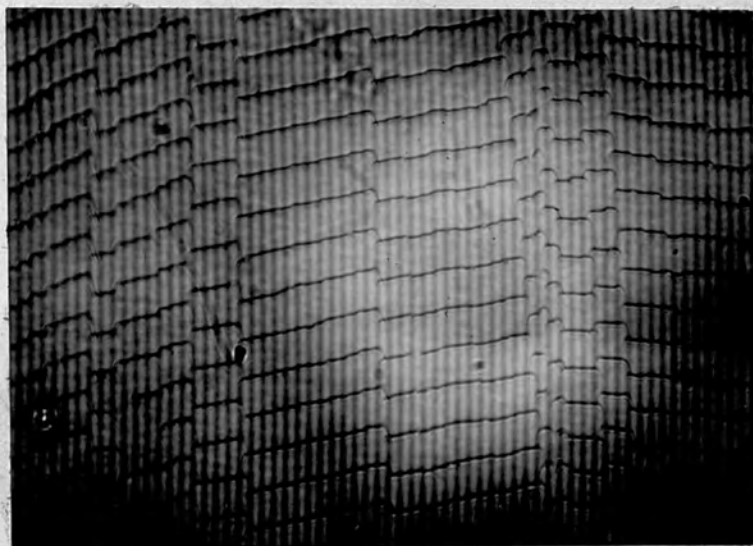


Figure 7. Multiple beam interferogram of a potassium bromide cleavage face x 50. ( $\lambda = 5461 \text{ \AA}$ ).

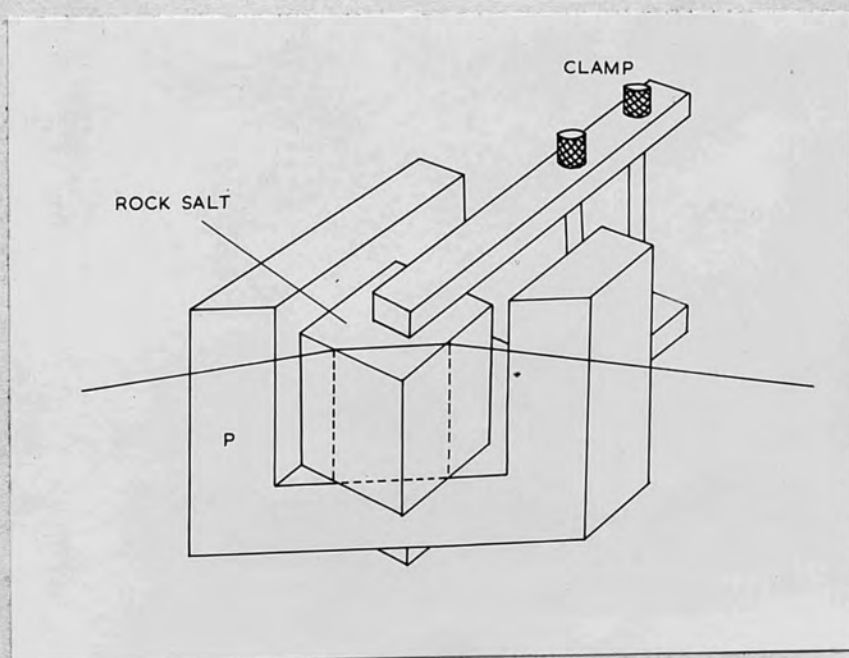


Figure 8. Jig used for cutting (110) faces of alkali halides.

orientation of the selenium overgrowth, a further polishing step had to be undertaken. A circular wax lap was prepared on a pitch base in the usual manner (Strong 1938)<sup>93</sup> and its surface made flat. Putty powder (Stannic oxide) from W. Canning and Co. Ltd., London, was used as the polishing medium after decanting three times from a suspension in water to remove the larger particles. A number of organic liquids were tried as lubricants for polishing but it was found that the best polish was obtained using a saturated solution in distilled water of the alkali halide to be polished.

The technique required to produce a good scratch free surface was found to vary from day to day, possibly due to changes in atmospheric humidity. Normally however the lap was rotated at about 10 revolutions per second, moistened with the lubricant and lightly powdered with the putty powder. The crystal was then moved lightly back and forth across the lap diameter. Polishing only occurred as the lap became almost dry. The next stage of polishing was performed on clean "Selvyt" cloth supported on plate glass. The cloth was first moistened with water free isopropyl alcohol, and the crystal polished with a circular motion to remove all traces of wax and putty powder. Then the crystal was transferred

to a piece of dry selvyt cloth polished again, and then immediately transferred to the vacuum chamber.

This process produces a very clean surface (Miller 1962)<sup>94</sup> which is highly reflective. On silvering and examining the surface with multiple beam Fizeau fringes a flat smooth surface was shown. The surface was not atomically smooth but local irregularities were little more than about 200 angstrom units in height (Figure 9).

The polishing of a crystal surface must introduce considerable disorder, or even an amorphous<sup>o</sup> layer, which would not be conducive to epitaxial growth. Prior to the evaporation of the film therefore the crystal was annealed in vacuum. This process apparently restores the monocrystallinity of the surface. The annealing temperatures required were approximately 400°C for one hour with rock salt, and 340 to 370°C for one hour with potassium bromide depending upon the face. These annealing temperatures varied quite considerably with different faces and also from crystal to crystal. Some difficulty was at first encountered in the selection of the right annealing temperatures for the different crystal surfaces. It was found that if the annealing temperature was too high appreciable thermal etching of the substrate took place leaving a very disturbed surface. If the



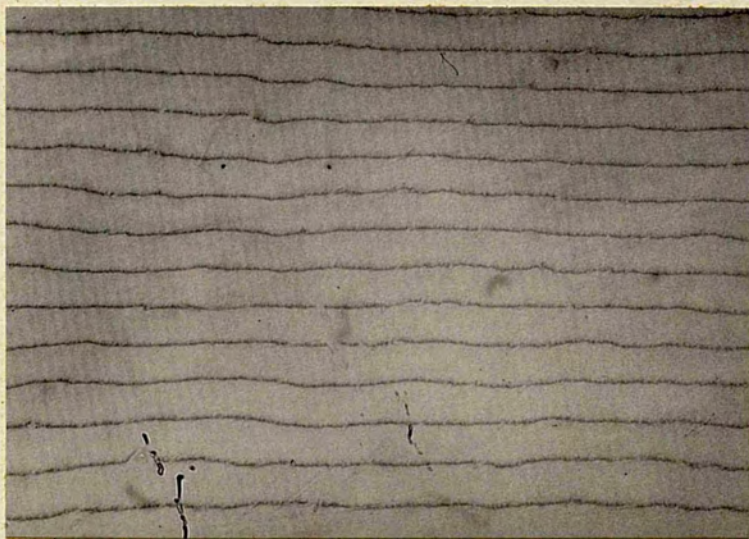


Figure 9. Multiple beam interferogram  
of a polished potassium bromide  
(100) face.  $\times 50$  ( $\lambda = 5461 \text{ \AA}$ ).



temperature was too low insufficient annealing occurred. Selenium films were therefore deposited on polished (100) faces of potassium bromide which had been etched at varying temperatures. Figures 10 and 11 show optical micrographs of potassium bromide (100) polished faces annealed at  $420^{\circ}\text{C}$  and  $370^{\circ}\text{C}$ , and figures 12 and 13 show the diffraction patterns of the films deposited on these surfaces. The same procedure was adopted for other polished crystal faces.

(c) Cleaved calcium fluoride, barium fluoride and magnesium oxide.

These crystals were again artificially grown, and those obtainable were of irregular shape. Their shape and relative hardness made it impossible to prepare freshly cleaved faces using the guillotine. A sharp straight edged blade cut at  $30^{\circ}$  was placed parallel to the cleavage planes, and then struck with a small hammer. This method produced quite flat faces, but as for the alkali halides these were crossed by numerous cleavage steps.

### 3.5. The deposition of films.

(a) The vacuum system.

The pumping system was built up from an "Edwards High Vacuum" single stage rotary pump type 1.8.50. backing a "Metropolitan Vickers" two stage, three inch





Figure 10. (100) potassium bromide surface  
annealed at  $420^{\circ}\text{C}$ .

Oblique illumination. x 200.



Figure 11. (100) potassium bromide surface  
annealed at  $370^{\circ}\text{C}$ .

Oblique illumination x 200.



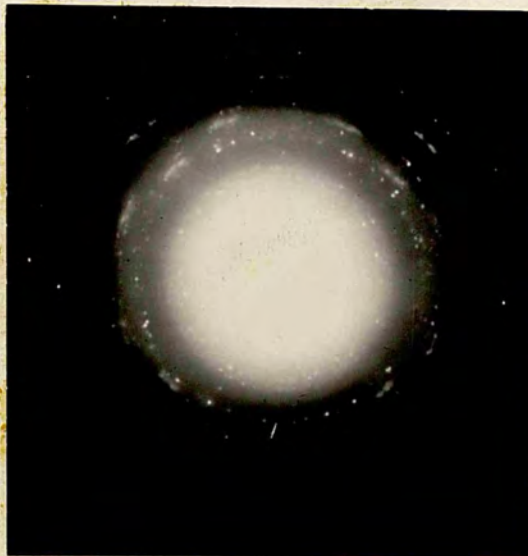


Figure 12. Diffraction pattern from  
Se film on surface annealed at  $420^{\circ}\text{C}$ .

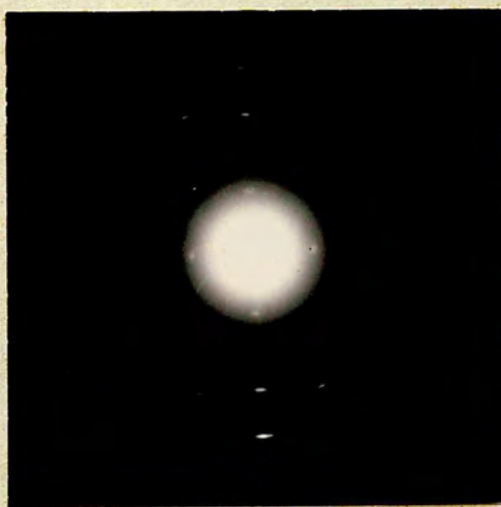


Figure 13. Diffraction pattern from  
Se film on surface annealed at  $370^{\circ}\text{C}$ .

oil diffusion pump. Between the rotary and diffusion pumps was connected a phosphorous pentoxide trap to remove water vapour from the system, together with a piping system which enabled the evaporation chamber to be pumped by the rotary and diffusion pump, or the rotary pump alone. Directly on top of the diffusion pump flap valve was mounted the base plate for the evaporation chamber.

Pressure measurement was by a discharge tube between the two pumps, and a "Genevac" type P.N.C.1. Penning gauge in the evaporation chamber. The Penning gauge was calibrated between  $10^{-3}$  and  $10^{-6}$  m.m./Hg.

(b) The evaporation chamber.

The base plate was machined from  $\frac{1}{4}$ " steel plate and sealed onto the diffusion pump with a neoprene "O" ring gasket. On top of this was mounted a 6" diameter x 2" high brass cylinder, and on top of this a 6" diameter x 8 inch high pyrex glass bell jar. These were sealed to one another and the base plate by Viton rubber gaskets. Electrical access to the apparatus inside the bell jar was provided by insulated terminals passing through the base plate for the evaporation filament, and through the brass cylinder for the substrate heater. The thermocouple wires were led directly through ceramic bushes in the brass cylinder and sealed with "Apieson" wax.



The disposition of the apparatus inside the evaporation chamber is shown in the diagram, Figure 6, and in the photograph, Figure 14. Just above the base plate in the aperture to the diffusion pump a stainless steel baffle was placed to minimize the amount of selenium getting through to the pump, and the backstreaming of oil to the evaporation chamber. The evaporation boat and filament were mounted just above the baffle, supported on the low tension supply leads. 9 c.m. above this was the substrate, held to the substrate heater by molybdenum straps. The substrate heater was constructed of a baked pyrophyllite base supporting a flat zig-zag of spirally wound 32 S.W.G. tungsten. The Stainless steel heater plate was separated from this heating element by a thin sheet of mica (see Figure 15). The area of the heating element and heater plate were made several times that of the substrate to ensure uniform heating. Mounted between the substrate and the vapour source was the shutter assembly, consisting of a stainless steel plate with a 1 c.m. diameter aperture and a stainless steel shutter plate. The shutter was actuated by a rod passing through a rotary seal in the base plate, and allowed the substrate to be shielded from the vapour source. 0 - 5 amps were supplied to the substrate heater from a variac with an ammeter in series, and 0 - 25 amps to the evaporation filament from a transformer and variac.



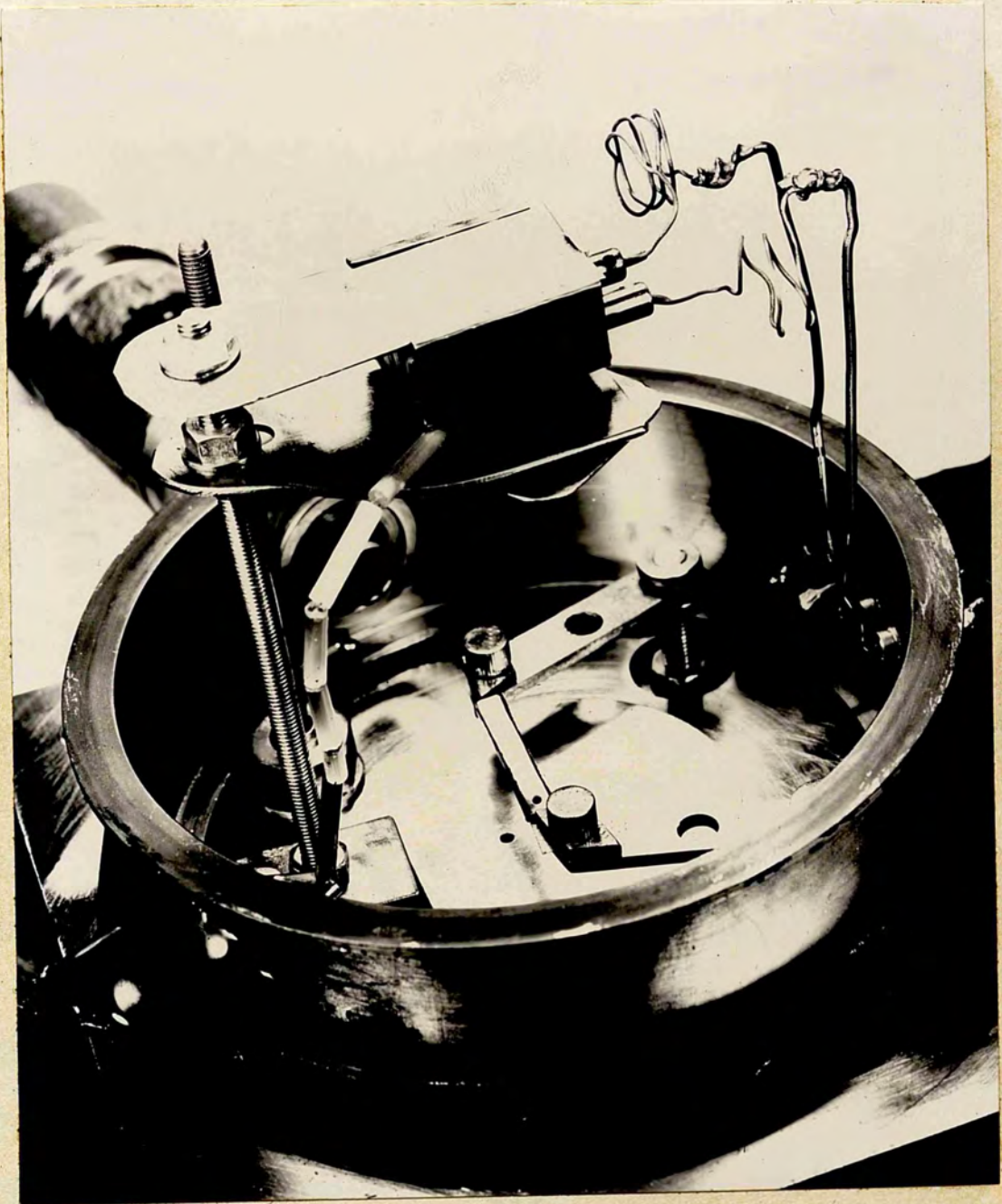


Figure 14. Evaporation chamber.

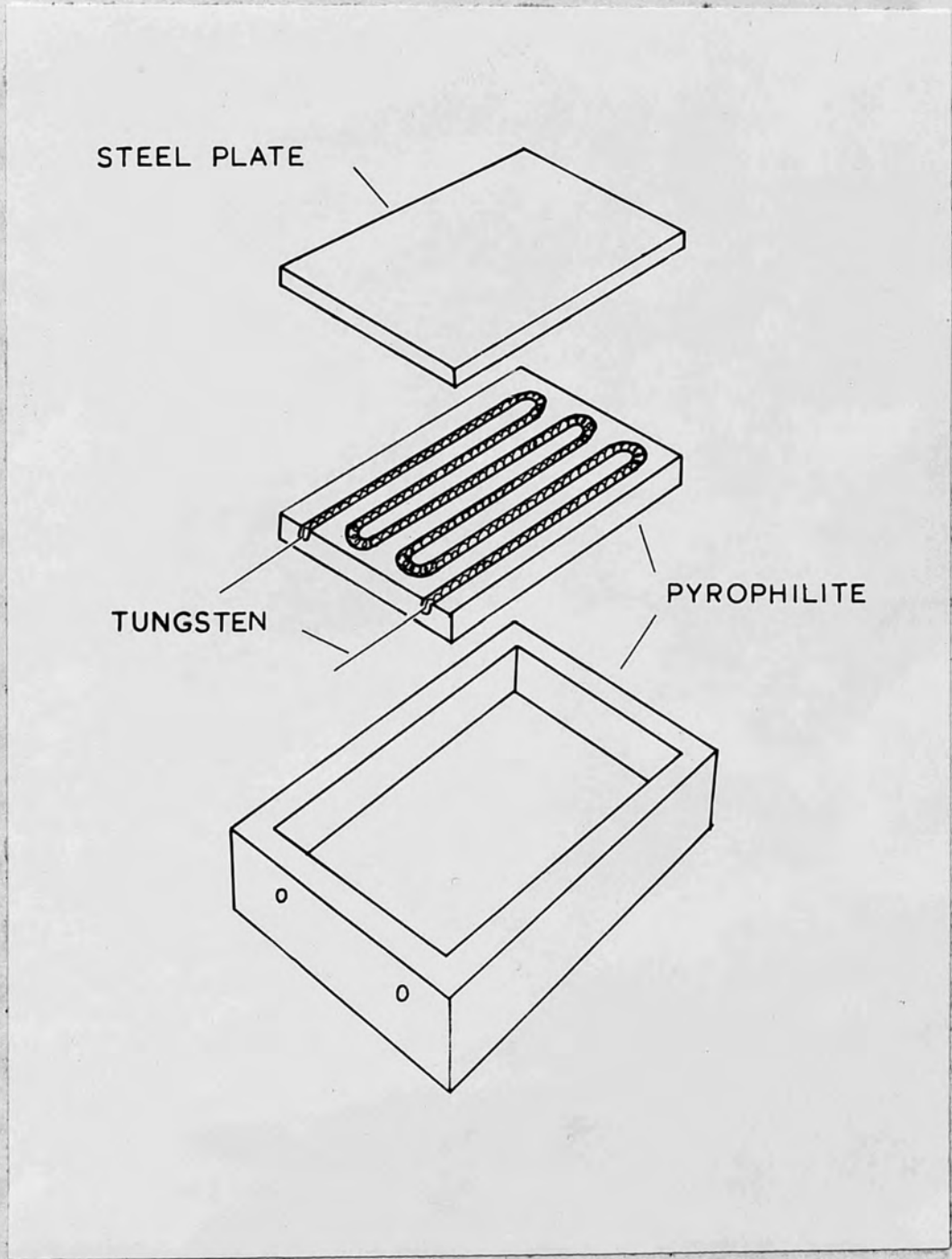


Figure 15. The substrate heater.



It was found necessary to thoroughly clean the evaporation chamber every third or fourth evaporation. Otherwise poorly oriented dirty films were obtained.

(c) Measurement of substrate temperature.

Temperature measurement was by means of a calibrated chromel-alumel thermocouple. This was made by flame welding 0.009" diameter chromel and alumel wires so that the junction formed was a sphere with a diameter of about 0.03". The cold junction was immersed in a flask containing water, with a mercury thermometer immediately adjacent to the junction. Potential measurements were made with a type 3378B Tinsley potentiometer. The twin bore quartz tubing which carried and insulated the thermocouple wires was clamped onto the shutter aperture plate below the substrate. This allowed the hot junction of the thermocouple to be sprung against the substrate surface.

Good thermal contact between the thermocouple junction and the substrate surface was ensured by the way in which the junction sank into the substrate surface during the time when the substrate was being annealed. Figure 16 shows the pit in the substrate surface left when the thermocouple was removed.

(d) Evaporation procedure.

The freshly prepared substrate was placed immediately on the heater plate, the shutter moved over it, and the evaporation chamber pumped out. While the



59



Figure 16. Pit left by thermocouple  
in substrate surface. x 50.

pumping was proceeding the current through the substrate heater was adjusted to give the required annealing temperature for the substrate. Cleaved substrates were also heated in this way to remove contamination and to discourage any further contamination by compounds present in the evaporation chamber. The heat generated by the substrate heater also assisted in the outgassing of the walls of the chamber.

After the annealing temperature had been maintained for one hour the temperature was adjusted to that required for film deposition. This caused the pressure to fall from a normal  $6 \times 10^{-5}$  m.m./Hg. at the end of annealing to  $2 \times 10^{-5}$  m.m./Hg. for film deposition.

While the substrate was cooling the evaporation boat filament was switched on and the selenium melted and outgassed. The temperature of the molten selenium was adjusted by means of a variac controlling the current supplied to the evaporation filament and allowed to reach an equilibrium value. When this had been reached the shutter was removed from the substrate surface, and the substrate exposed to the vapour beam. Film thicknesses for any given surface were roughly proportional to the time of exposure to the vapour beam.



It was found that if the film and substrate were allowed to cool to room temperature in the evaporation chamber, agglomeration of the deposit occurred. The substrate and film were therefore removed hot from the chamber and cooled more quickly in a dessicator.

### 3.6. Removal of films from the substrates.

The removal of films from their substrates was necessary in order to examine them in the electron microscope. This meant that solvents were required which would dissolve away the substrate and allow the film to float off, without reacting with the film. The alkali halides were relatively easy to deal with as they are soluble in water. A number of solvents were tried for barium fluoride, calcium fluoride and magnesium oxide but 35% hydrochloric acid was the only one found to be satisfactory.

Some difficulty was experienced with non continuous films tending to break up on floating off from the substrate. It was therefore found necessary to reinforce all films with a thin electron transparent carbon film. Approximately 200Å of carbon were deposited on top of the selenium still on the substrate by evaporation from an electric arc at a vacuum of about  $5 \times 10^{-5}$  m.m./Hg. This allowed the fragile films to be handled without any danger of break up.

one hour for barium fluoride to twenty four hours for calcium fluoride. Although the films were found from



(a) Removal from Alkali halides.

The substrate and film were lowered gently into distilled water to which had been added a few drops of ethyl alcohol to reduce the surface tension. Care was taken to hold the substrate at a small angle to the water so that the water seeped around and underneath the film. Eventually the water separated the film from the substrate, and the film floated freely on the water surface. The film was then picked up on a clean glass cover slip and transferred to another dish of distilled water to remove traces of alkali halide solution. Small pieces of the film were now picked up on electron microscope grids, and when dry examined in the microscope.

(b) Removal from barium fluoride, calcium fluoride and magnesium oxide.

The solvent used for these substrates was 35% hydrochloric acid. Substrates with films were placed on the bottom of shallow dishes and the solvent poured in until the level was such that only surface tension prevented it from covering the substrate. The dishes were then left covered overnight, and during this time the acid slowly seeped between the film and substrate. The time required to free the film varied from about one hour for barium fluoride to twenty four hours for calcium fluoride. Although the films were freed from

the substrates very little dissolution of the mass of the substrate occurred. From this stage the films were treated as those on the alkali halides.

22. Holland J. (1931), *Viscosity Dependence of Thin Films*  
(Chapman and Hall, London).

23. Holmboe S. (1945), *Multiple Beam Interferometry*  
(Oxford - Clarendon).

24. Young, (1933), *Modern Physical Laboratory Practice*.  
(Blackie - London).

25. Miller R.S. (1933) Ph.D. Thesis, London University.

### References to Chapter 3.

91. Holland L. (1956), *Vacuum Deposition of Thin Films* (Chapman and Hall, London).
92. Tolansky S. (1948), *Multiple Beam Interferometry* (Oxford - Clarendon).
93. Strong, (1938), *Modern Physical Laboratory Practice*. (Blackie - London).
94. Miller R.F. (1962) Ph'd. Thesis. London University.

Crystal orientation was examined by the diffraction of transmitted electrons, the area contributing to the pattern being in the order of a micron in diameter. Due to the low melting point of selenium great care had to be taken not to use too high an electron beam intensity, otherwise melting and evaporation of the film occurred. Electron micrographs of specimens were examined at electronic magnifications of up to 10,000, magnification being calibrated by reference to the squares on the microscope grid. The magnification available was restricted again by the melting point of the selenium, making examination of the microstructure of the films difficult.



Chapter 4. Electron diffraction and micrography of films.

4.1. Introduction.

The structure of films grown by the methods outlined in Chapter 3 were investigated using transmission electron microscopy and diffraction. The microscope used was a Metropolitan Vickers E.M.3., the magnetic optical system of which comprises a single condenser lens, an objective, and two projectors. An electron accelerating voltage of 75 Kv. was used, the object was to look for evidence of epitaxial growth of the selenium films, and if it occurred to investigate more closely the structure and orientation of the films.

Crystal orientation was examined by the diffraction of transmitted electrons, the area contributing to the pattern being in the order of a micron in diameter. Due to the low melting point of selenium great care had to be taken not to use too high an electron beam intensity, otherwise melting and evaporation of the film occurred. Electron micrographs of specimens were examined at electronic magnifications of up to 10,000, magnification being calibrated by reference to the squares on the microscope grid. The magnification usable was restricted again by the melting point of the selenium, making examination of the microstructure of the films difficult.

floating off the film from the substrate this edge was laid on the microscope grid parallel to the grid bars

Calibration of the diffraction patterns was accomplished by evaporating a film of sodium chloride on top of the selenium to give a combined diffraction pattern. Selenium and carbon films were mounted on a microscope grid and sodium chloride evaporated on to this surface from a tungsten filament. This gave a pattern made up of sodium chloride rings and the selenium spot pattern. The thickness of sodium chloride required varied with the thickness of the selenium film and had to be adjusted so that it did not mask the weaker selenium reflections.

Where epitaxial growth of selenium occurred the relative orientations of the film and substrate were very important. An attempt was made to obtain superimposed film and substrate reflection diffraction patterns from substrate surfaces with half their area covered with selenium crystallites. This however was abandoned due to electrostatic charging of the surface distorting the electron beam.

The problem was finally solved with the help of microscope grids with rectangular apertures (100/400 mesh). After evaporation of the film and carbon support, the substrates were cleaved in a known direction cutting the face. This gave a sharp straight edge to the film. After floating off the film from the substrate this edge was laid on the microscope grid parallel to the grid bars

making up the short sides of the apertures. Thus the substrate orientation was known in terms of the grid orientation. Having obtained a diffraction pattern from the film in the electron microscope, it was possible by reducing the power of the objective lens, to throw a shadowgraph of the grid bars on top of the diffraction pattern. This gave directly the relationship of the selenium diffraction pattern to the known direction in the substrate surface.

Although it was not possible to rigorously examine all the factors affecting the growth of films, the general influence of some of the more easily variable conditions was investigated.

While the sequence of micrographs and diffraction patterns shown are "typical", both microstructure and orientation varied even for films grown under apparently identical conditions. This throws some doubt on the uniformity of the structure of the single crystal substrates obtained, but may also be due to some factor not controlled in the experimental procedure. It must also be pointed out that the observations were made on films after cooling, stripping from the substrate, and mounting on grids. Such processes were carried out with a great deal of care, but might well disturb the orientation of the films.



All thicknesses quoted are mean thicknesses, i.e. those which the films would have if they were reduced to continuous parallel sided layers. (See Chapter 5.)

#### 4.2. Selenium films on sodium chloride (rock salt).

##### (a) Cleaved (100) sodium chloride.

Selenium films were deposited on cleaved (100) sodium chloride substrates at temperatures between 60 and 115°C, with deposition rates which varied from 200 to 1000Å/minute. Above 115°C selenium did not condense on the substrate and no film was formed. The thickness of the films varied from 200 to 2000Å.

Electron diffraction patterns of these films showed that the structure changed from completely amorphous at a substrate temperature of 70°C to polycrystalline hexagonal at 80°C. This polycrystalline structure did not change appreciably on increasing the substrate temperature to 115°C, and no tendency towards epitaxial growth was observed over any portion of the temperature range.

A typical film condensed on a substrate at 95°C with a mean thickness of 2000Å is shown in the micrograph Figure 17. Individual crystallites in this film appear fairly large, and the diffraction pattern (Figure 18) shows a non uniform intensity distribution around the rings as a consequence of these small oriented areas.

(b) Polished (110) sodium chloride.

Selenium was deposited on polished (110) sodium chloride at substrate temperatures of 80 and 105°C, and deposition rates of 200 and 500 Å/minute. The mean thickness of these films was approximately 700Å. Electron diffraction from the films gave a polycrystalline hexagonal ring pattern very similar to that from cleaved sodium chloride, although the crystallites were smaller in this case. The micrograph and diffraction pattern (Figures 19 and 20) were obtained from a typical film formed at a substrate temperature of 105°C.

(c) Polished (111) sodium chloride.

Selenium was deposited on polished (111) sodium chloride at substrate temperatures of 80 and 100°C with a deposition rate of 200Å/minute. The films so produced had a mean thickness of 500Å.

Electron diffraction from the films again gave the pattern of a polycrystalline hexagonal film very similar to that obtained from films on cleaved sodium chloride. Figures 21, and 22 show the electron micrograph and diffraction pattern of a film condensed onto (111) sodium chloride at 100°C.





Figure 17. Selenium on (100) Na Cl x 8000.  
2000 Å thickness.

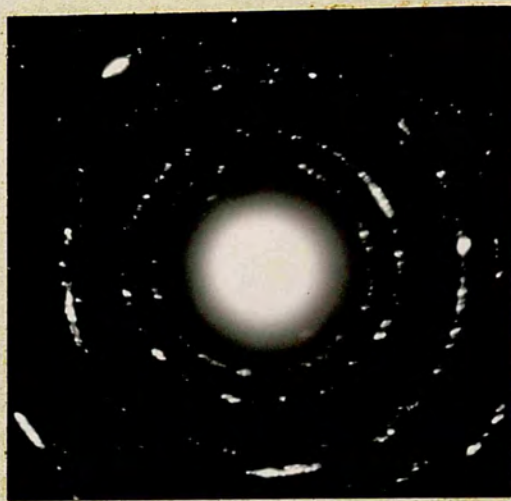


Figure 18. Diffraction pattern from  
selenium on (100) Na Cl.





Figure 19. Selenium on (110) Na Cl x 8000  
700 Å thickness.



Figure 20. Diffraction pattern from  
selenium on (110) Na Cl.





Figure 21. Selenium on (111) Na Cl x 8000.  
500 Å thickness.



Figure 22. Diffraction pattern from  
selenium on (111) Na Cl.

(d) The diffraction pattern given by selenium on (100), (110), and (111) sodium chloride.

The diffraction patterns given by polycrystalline hexagonal selenium deposited on the three faces of sodium chloride were very similar, the same diffraction rings being given by all three films. By evaporating a thin polycrystalline film of sodium chloride on top of the selenium film (see Chapter 4.1), and obtaining two superimposed diffraction patterns, it was possible to calibrate the selenium pattern (Chapter 4.3(a)). The indices of the selenium rings were then calculated with the aid of a reciprocal lattice model for hexagonal selenium. A diagram giving these indices is shown in Figure 23.

#### 4.3. Selenium films on (100) potassium bromide.

Selenium films were prepared on a number of cleaved and polished potassium bromide surfaces which were maintained at temperatures from  $78^{\circ}$  to  $102^{\circ}\text{C}$ . The cleaved substrates had previously been annealed at  $340^{\circ}\text{C}$ , and the polished ones at  $350$  to  $375^{\circ}\text{C}$  to reduce strain and restore the monocrystallinity of the surface. The mean thickness of the films was varied from 270 to  $3000\text{\AA}$ .

Epitaxial growth of selenium was observed over a substrate temperature range of  $83$  to  $102^{\circ}\text{C}$ , and over the



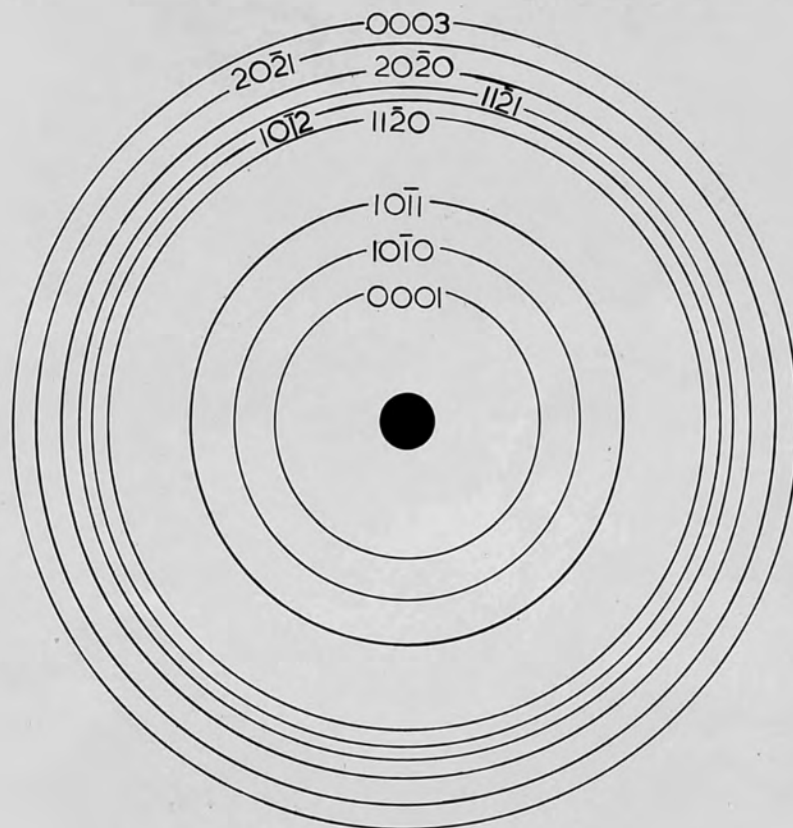


FIG. 23. DIAGRAM OF ELECTRON DIFFRACTION PATTERN FROM SELENIUM DEPOSITED ON SODIUM CHLORIDE.

whole range of deposition rates. At  $78^{\circ}\text{C}$  the deposited film was found to be amorphous, and above  $102^{\circ}\text{C}$ , at the evaporation rates used, no film condensed on the substrate in 5 minutes. The micrograph, Figure 24, is typical of the <sup>form</sup> type of crystallites formed on the cleaved (100) potassium bromide surface. It shows that at a mean thickness of  $1500\text{\AA}$  the film is not continuous but consists of patches or islands of selenium crystallites already in the region of  $2,500\text{\AA}$  thick. These islands are growing outwards in the plane of the substrate surface in the form of small needle-like crystals which appear to be hexagonal prisms. This is confirmed by the diffraction pattern.

Between the larger islands are small doughnut shaped islands. The bare patches in the centre of these islands are difficult to explain on the basis of a completely flat substrate surface. They might be due to selenium nucleating around the edge of small plateaus of potassium bromide above the main surface, formed when cleaving. It seems more likely however that hopper type etch pits have formed in the surface during the annealing process, and the selenium has nucleated on a step inside the pit and grown back over the edge onto the main substrate surface.

The diffraction pattern shown in Figure 25 is again typical of that given by selenium films on (100) potassium bromide. The four inner spots although easily seen on the plate are barely visible on the print.

(a) Analysis of the diffraction pattern.

Although the diffraction pattern shown in Figure 25 was expected to be that of the hexagonal selenium lattice, at first sight it showed no relation to any plane through the reciprocal lattice. However the micrograph of the film giving this pattern shows needle-like crystals whose long axes appear to be oriented in two directions at  $90^\circ$  to one another. It was then found that the diffraction pattern could be split into two primary patterns which were superimposed also at  $90^\circ$  to one another.

The primary pattern was seen to be similar in form to the array of reciprocal lattice points obtained by taking a plane through the origin of the reciprocal lattice with the zone axis  $10\bar{1}0$ . (Figure 26). This would then mean that the hexagonal selenium  $(10\bar{1}0)$  plane was perpendicular to the electron beam, and the C axis oriented in two directions at an angle of  $90^\circ$ . The diffraction pattern predicted from the reciprocal lattice for selenium oriented in this way (Figure 27) appeared to be almost identical with the experimentally observed pattern. Only four extremely faint spots lying between the proposed 0001 and 0002 type reflections remained





Figure 24. Selenium on (100) K Br. x 8000.

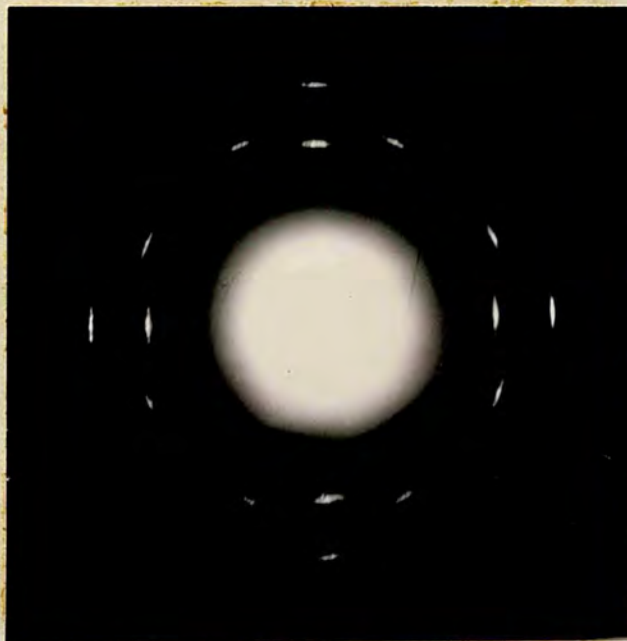
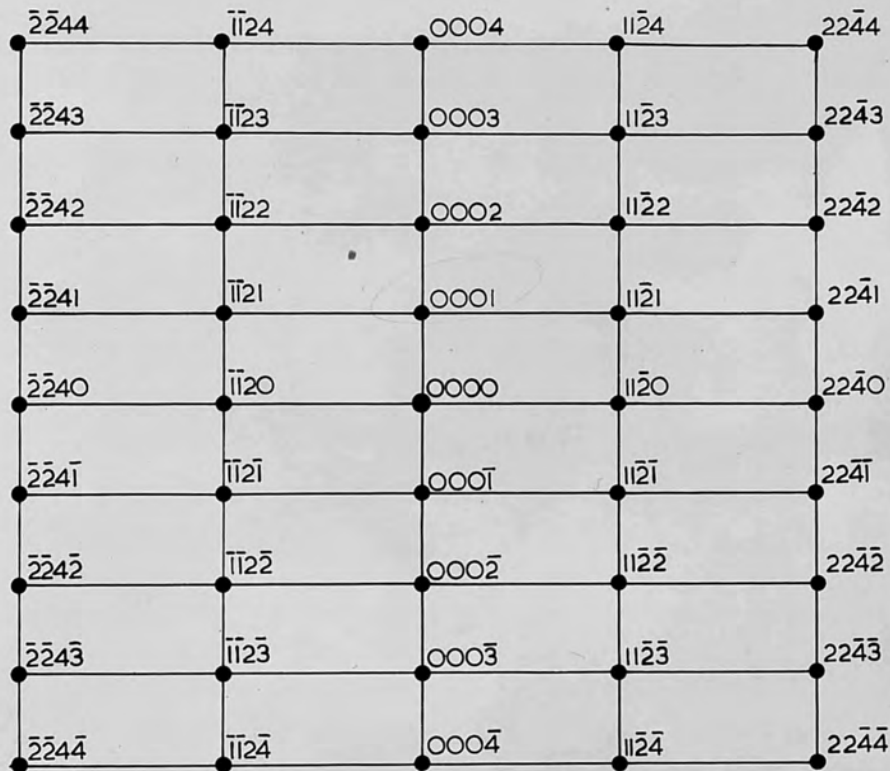


Figure 25. Diffraction pattern from selenium on (100) K Br.



Out  
forbidden  
spot.

RECIPROCAL LATTICE FOR HEXAGONAL SELENIUM CRYSTAL:  
PLANE THROUGH THE ORIGIN, WITH ZONE AXIS  $10\bar{1}0$

Figure 26.



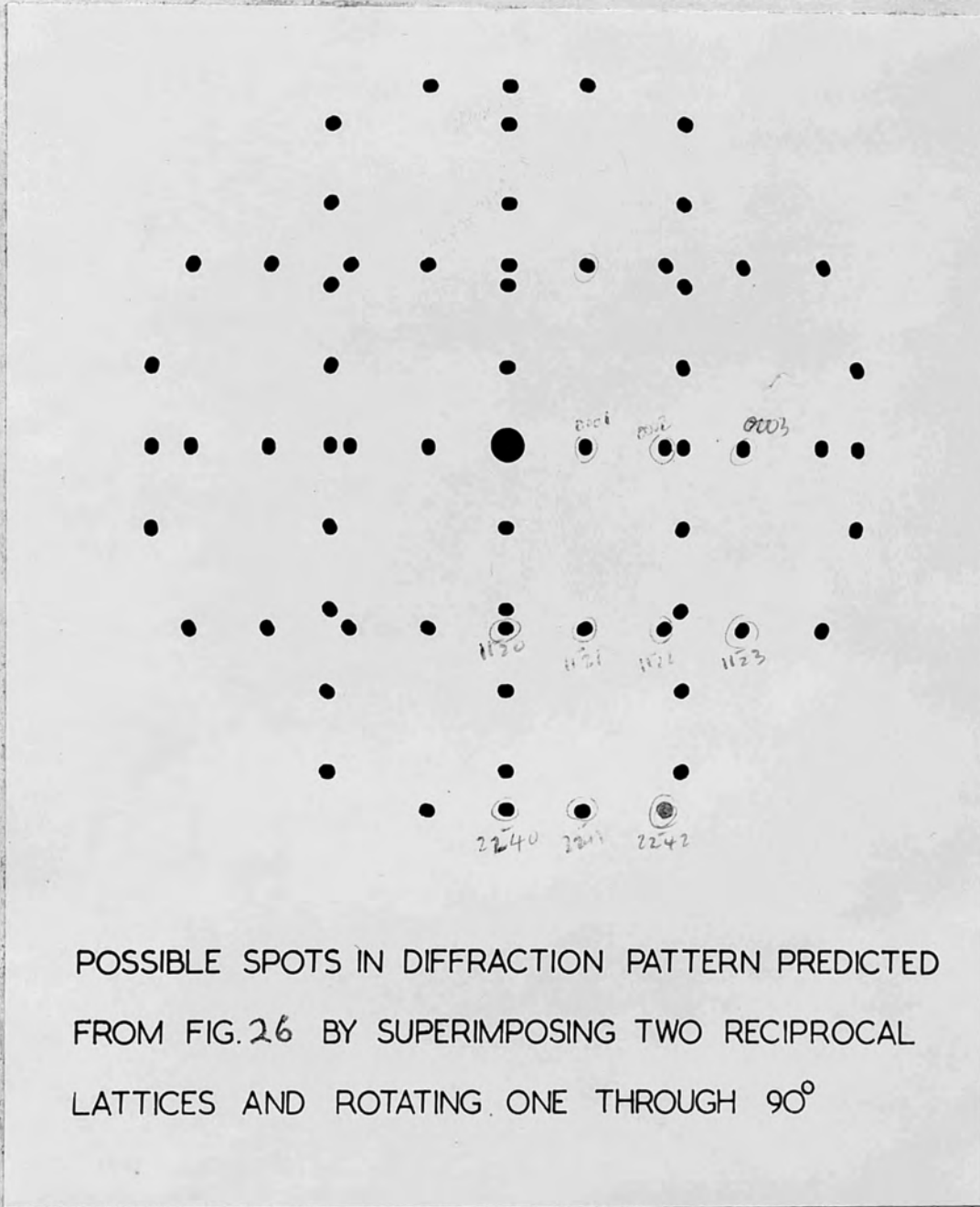


Figure 27.

Indices



unaccounted for, and these appeared to be 1011 type reflections.

The positive identification of the selenium diffraction spots was established by calibration of the diffraction pattern with a superimposed sodium chloride pattern as shown in Figure 28. (see Chapter 4.1).

Using the expression,

$$n \lambda = 2d \sin \theta \quad (\text{Bragg equ'}) \quad (1)$$

Where  $n$  is an integer,  $\lambda$  is the wavelength,  $d$  is the planar spacing, and  $\theta$  is the angle of the diffracted beam, then if  $\theta$  is small enough

$$2d \theta = \lambda .$$

If  $L$  is the length of the normal from the crystal to the recording plate in the diffraction camera, and  $r$  the radius of the diffraction ring, then

$$2 \theta = \frac{r}{L} \quad (2)$$

Combining (1) and (2)

$$d.r. = (\lambda .L.) \quad (3)$$

$$\text{and } d = \frac{(\lambda .L.)}{r} \quad (4)$$

The mean value of  $(\lambda .L.)$  was calculated for the sodium chloride 200, 220, 222, 400, and 422 reflections. As the two superimposed diffraction patterns were photographed simultaneously on the same plate this value of  $(\lambda .L.)$  was common to both. Thus having measured  $r$  for the spots on the selenium pattern it was possible to calculate  $d$

from equation (4).

Values of  $d$  calculated for the postulated 0001 and 11 $\bar{2}$ 0 type reflections were 4.93 and 2.18 $\text{\AA}$  respectively (actual values are 4.9495 and 2.1776 $\text{\AA}$ ). This confirmed the original deduction that the (10 $\bar{1}$ 0) plane was perpendicular to the electron beam, and also that the indexing of the diffraction pattern given in Figure 26 was correct. As the selenium film was mounted at 90 $^{\circ}$  to the electron beam in the diffraction camera, this also meant that the selenium crystals in the film had grown with their (10 $\bar{1}$ 0) or prism faces parallel with the (100) face of the potassium bromide. Also the selenium C axis was oriented in two directions at an angle of 90 $^{\circ}$  parallel to the substrate surface.

The value of  $d$  calculated for the postulated 10 $\bar{1}$ 1 type reflections was 3.01 $\text{\AA}$  (the actual value is 3.0000 $\text{\AA}$ ), which confirms that these are the 10 $\bar{1}$ 1 type reflections, (01 $\bar{1}$ 1) selenium plane parallel to the substrate surface).

In many of the diffraction patterns of the type shown in Figure 25 splitting of the diffraction spots had occurred. This was particularly evident with the 0001 reflections. As the films consist to quite a considerable extent of small regularly shaped crystallites, it is possible for the points in the reciprocal lattice

to have horns which protrude in the direction of least crystallite size in real space. When the Ewald sphere passes near such points it can intersect these horns and produce two spots where one would be expected. The displacement of these twin spots in the diffraction patterns from the positions of the expected spot is however proportional to the distance from the origin. If the above explanation was correct a much larger increase in displacement would be expected, and also, in the case of the  $1\bar{1}20$  reflections the twin spots would be displaced in a direction at  $90^\circ$  to that observed.

*double*  
}

It seems more likely therefor that the twin spots are produced by small areas of the film slightly misoriented with respect to one another. This could be caused by slight variations of the axial directions in the substrate, or by the process of stripping the film from the substrate.

(b) Orientation of selenium on the substrate.

The orientation of the selenium with respect to that of the substrate was established using the method described in Chapter 4.1. In this case the substrate and film were cleaved parallel to the substrate (010) face, to give the straight reference edge to the film. Figure 29 shows the film diffraction pattern with the superimposed grid bars. Some of the diffraction spot resolution was lost, but the direction of the grid bars with respect to the pattern



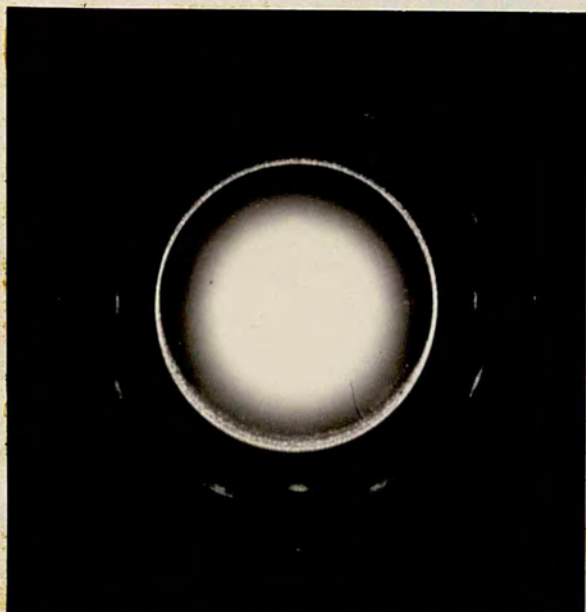


Figure 28. Diffraction pattern from Se film  
with superimposed Na Cl pattern.

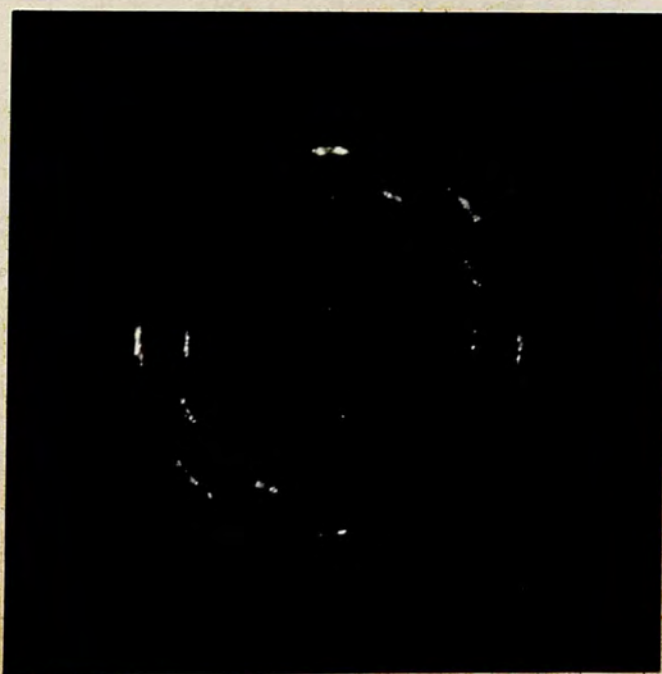


Figure 29. Diffraction pattern from Se film  
with superimposed grid bars.

is quite clear.

As the grid bars are parallel with the potassium bromide cube edge, and the selenium crystallographic directions are the same in real and reciprocal space, then the photograph shows the two selenium  $[0001]$  directions to be at  $90^\circ$  and to be bisected by the substrate  $[001]$  direction. This means that the selenium  $(10\bar{1}0)$  face was parallel to the substrate  $(100)$  face, and the selenium  $[0001]$  directions were parallel to the substrate  $[110]$  directions.

(c) Influence of substrate temperature.

The influence of substrate temperature on the structure of selenium films on cleaved potassium bromide was investigated with films of  $1000\text{\AA}$  mean thickness prepared at a deposition rate of approximately  $200\text{\AA}/\text{minute}$ . It was found that at  $78^\circ\text{C}$  and below the films prepared were amorphous, and above  $102^\circ\text{C}$  no deposition on the substrate surface occurred at the evaporation rates used. Micrographs and diffraction patterns from films prepared at  $100^\circ\text{C}$ ,  $95^\circ$ , and  $83^\circ\text{C}$  are shown in Figure 30, (a), (b) and (c), and Figure 31, (a), (b), and (c).

As previously stated the microstructure of films varied over film area, and particularly so in the case of cleaved surfaces. The only general tendency observed was for the growth of individual needle crystals to become less



pronounced as the temperature decreased. Although individual needles were still easily visible at the lowest temperature, they had a much finer structure. The diffraction patterns show that the greatest degree of orientation was found at  $100^{\circ}\text{C}$ , the orientation falling off slightly with decrease in temperature. At  $83^{\circ}\text{C}$  however, although very faint rings are visible, the films are still quite well oriented. Some splitting of the diffraction spots can be seen in pattern from the latter film, due probably to small changes in orientation from one small island of crystallites to another.

(d) Influence of film thickness.

The influence of increasing film thickness on orientation was investigated at a deposition rate of  $200\text{\AA}/\text{minute}$  with a substrate temperature of  $100^{\circ}\text{C}$ . No marked change in the degree of orientation was found from  $240\text{\AA}$  up to  $3000\text{\AA}$  mean thickness. The diffraction spots from the  $3000\text{\AA}$  film are more diffuse than those from the  $240\text{\AA}$  film and there is some splitting of the spots. However even at  $3000\text{\AA}$  the film is still well oriented (see Figures 33 and 34). Above  $3000\text{\AA}$  the films became continuous but the background of scattered electrons masked the diffraction pattern.

(e) Influence of deposition rate.

well oriented film, the diffraction pattern (Figure 35b)



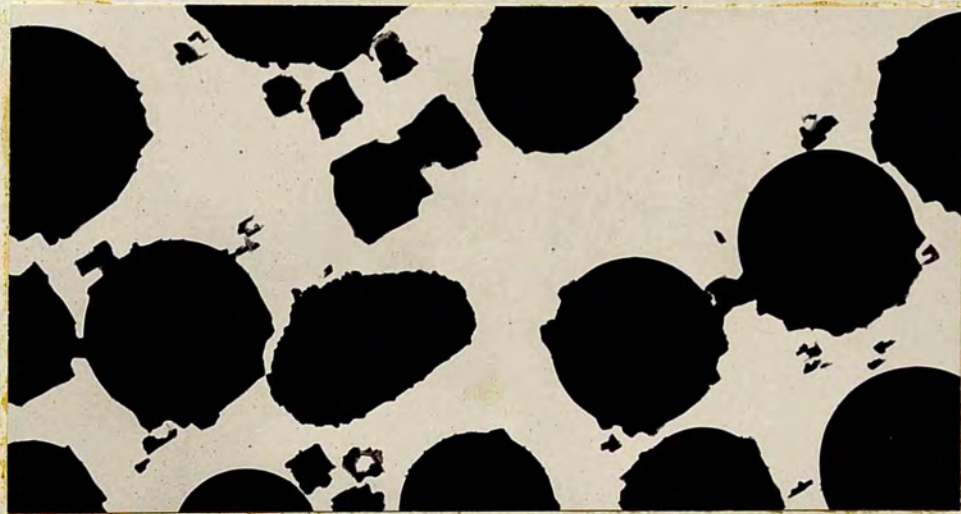
The increase of the deposition rate of selenium to  $1200\text{\AA}/\text{minute}$  still produced well oriented films at a substrate temperature of  $92^{\circ}\text{C}$ . Although no consistent change in size of the islands of oriented material was noticed their general shape did alter. The micrograph, Figure 34(a) shows the almost circular shape of the selenium islands which look very like liquid droplets. They were however very well oriented as, the diffraction pattern (Figure 34b) shows.

(f) Selenium deposited on polished (100) potassium bromide.

Cleavage faces of potassium bromide were polished using the method described in Chapter 3, and annealed at  $370^{\circ}\text{C}$  before film deposition. The type of surface obtained after annealing is shown in Figure 11, and is seen to be by no means flat on a micro scale. Selenium deposited on this surface at  $95^{\circ}\text{C}$  with a deposition rate of  $200\text{\AA}/\text{min}$  gave at  $320\text{\AA}$  mean thickness the surface decoration pattern shown in Figure 35(a). The circular decoration features are of the same size scale as the etch features shown in the optical micrograph of the substrate surface, and it is probable that they are due solely to these surface irregularities. Although it might be expected that such an irregular surface would not support the growth of a well oriented film, the diffraction pattern (Figure 35b)



(a)  
100°C



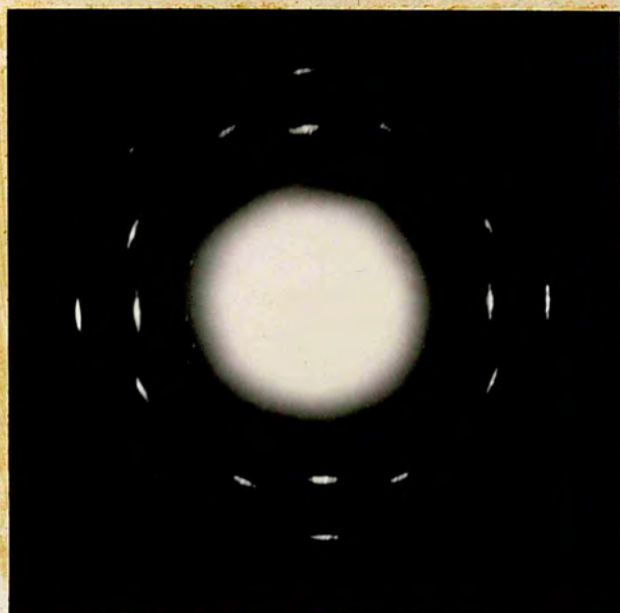
(b)  
95°C



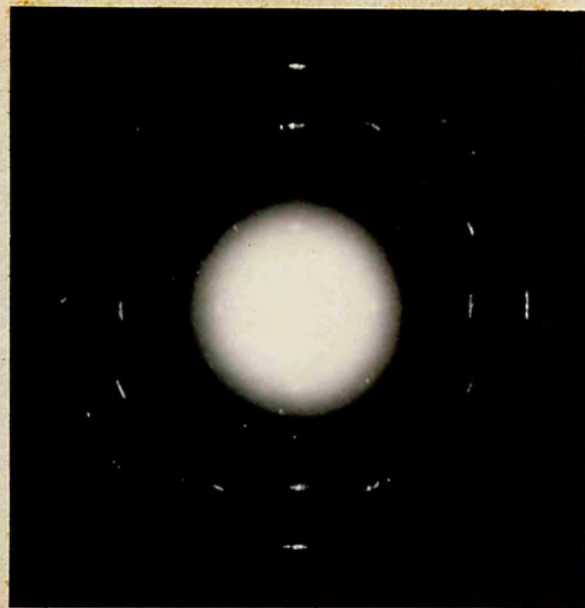
(c)  
83°C

Figure 30. The influence of substrate temperature on the growth of selenium on (100) cleaved K Br. x 8000.

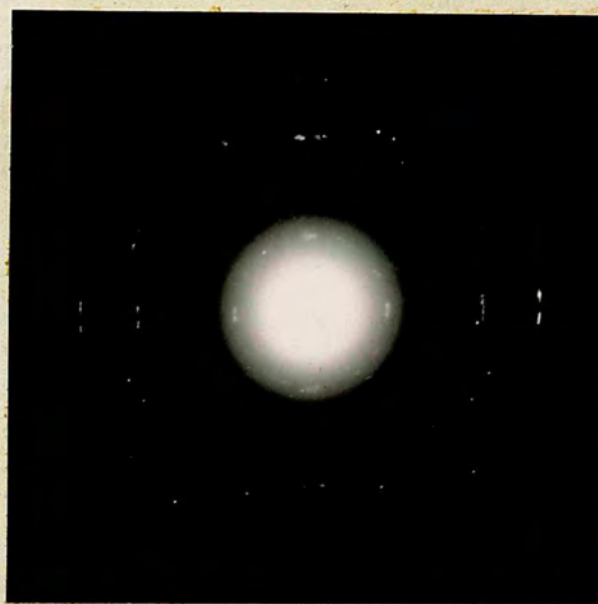




(a) 100°C



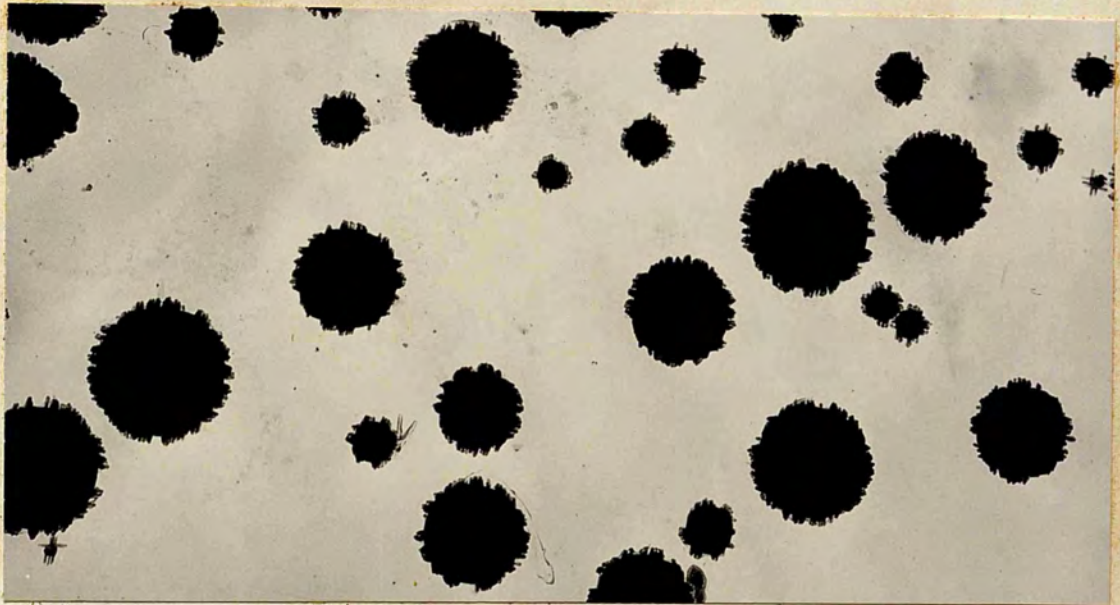
(b) 95°C



(c) 83°C

Figure 31. Diffraction patterns from selenium films grown on (100) cleaved K Br at different temperatures.





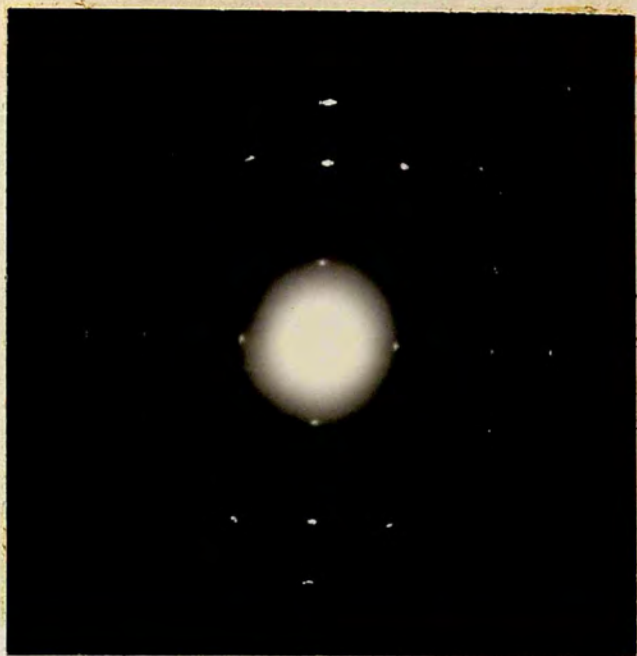
(a) Mean thickness 240 Å.



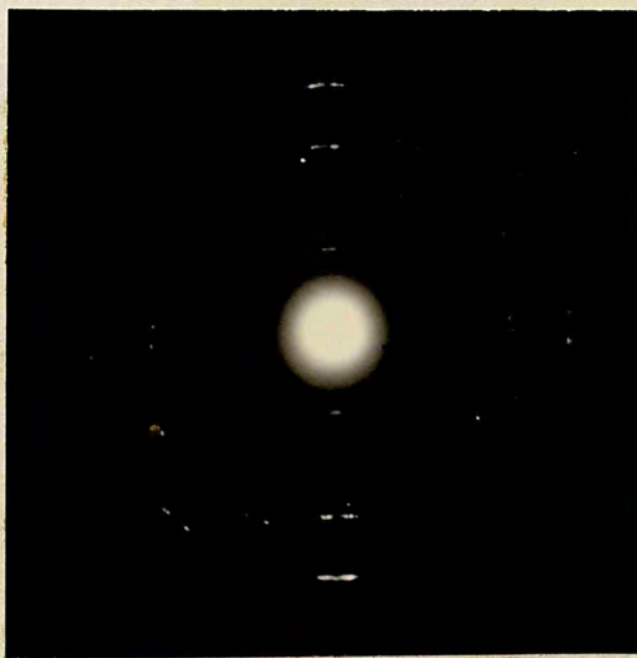
(b) Mean thickness 3000 Å.

Figure 32. Influence of film thickness on orientation of Se on (100) K Br. x 8000.





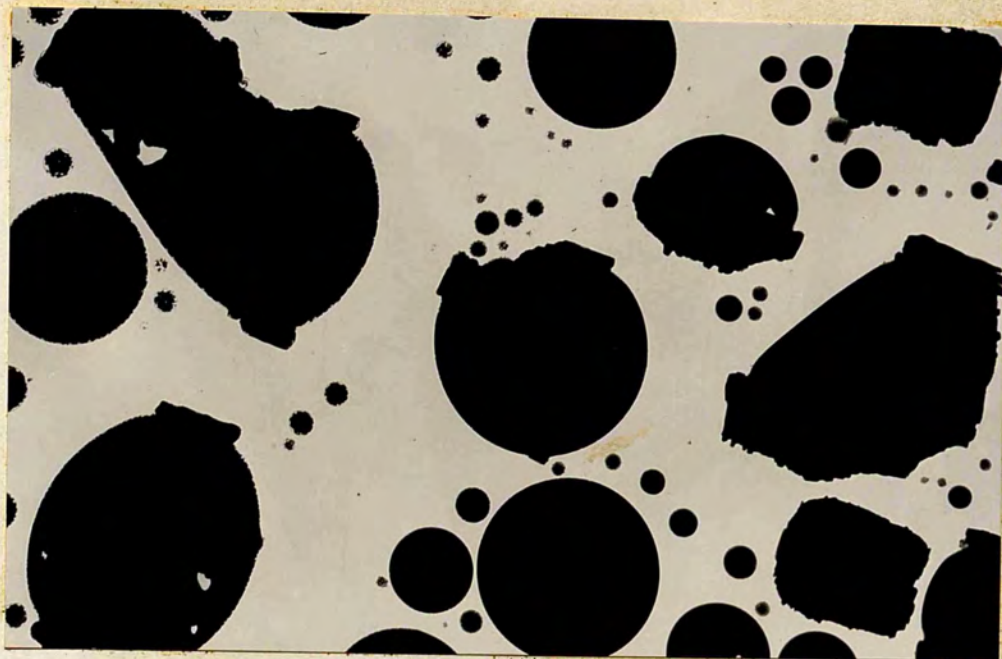
(a) Mean thickness 240 Å.



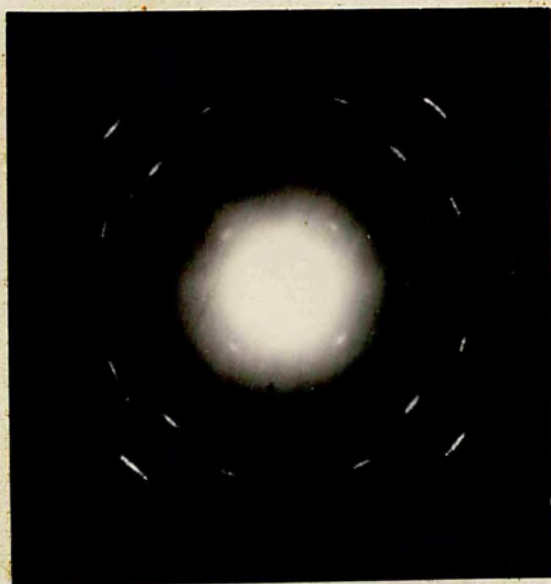
(b) Mean thickness 3000 Å.

Figure 33. Diffraction patterns showing the influence of thickness on the orientation of Se on (100) K Br.





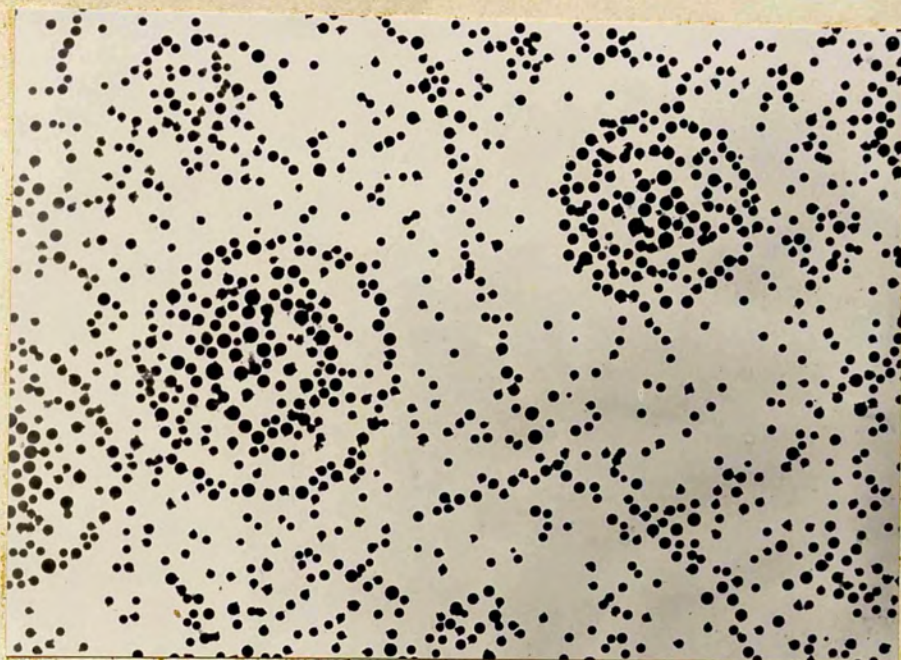
(a) Selenium deposited at  $1200\text{\AA}/\text{min.}$  x 8000.



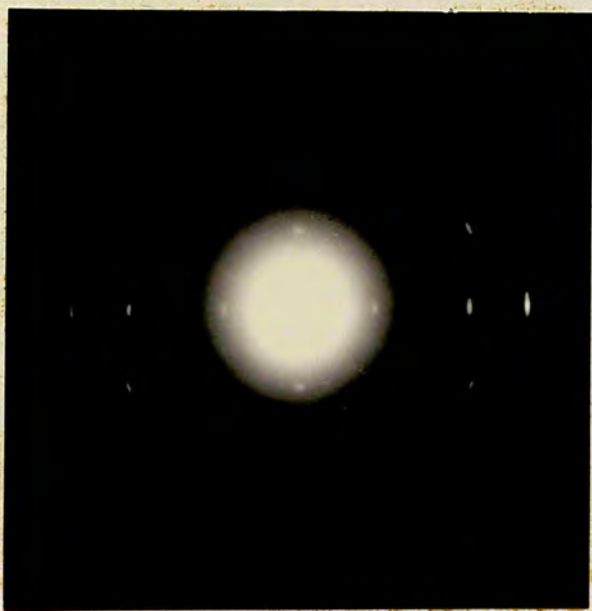
(b) Diffraction pattern from Se deposited at  
 $1200\text{\AA}/\text{min.}$

Figure 34. The effect of increasing the deposition rate of Se on (100) K Br. to  $1200\text{\AA}/\text{minute.}$





(a) Electron micrograph x 750.



(b) Diffraction pattern.

Figure 35. Se on polished (100) K Br.  $320\text{\AA}$   
mean thickness.



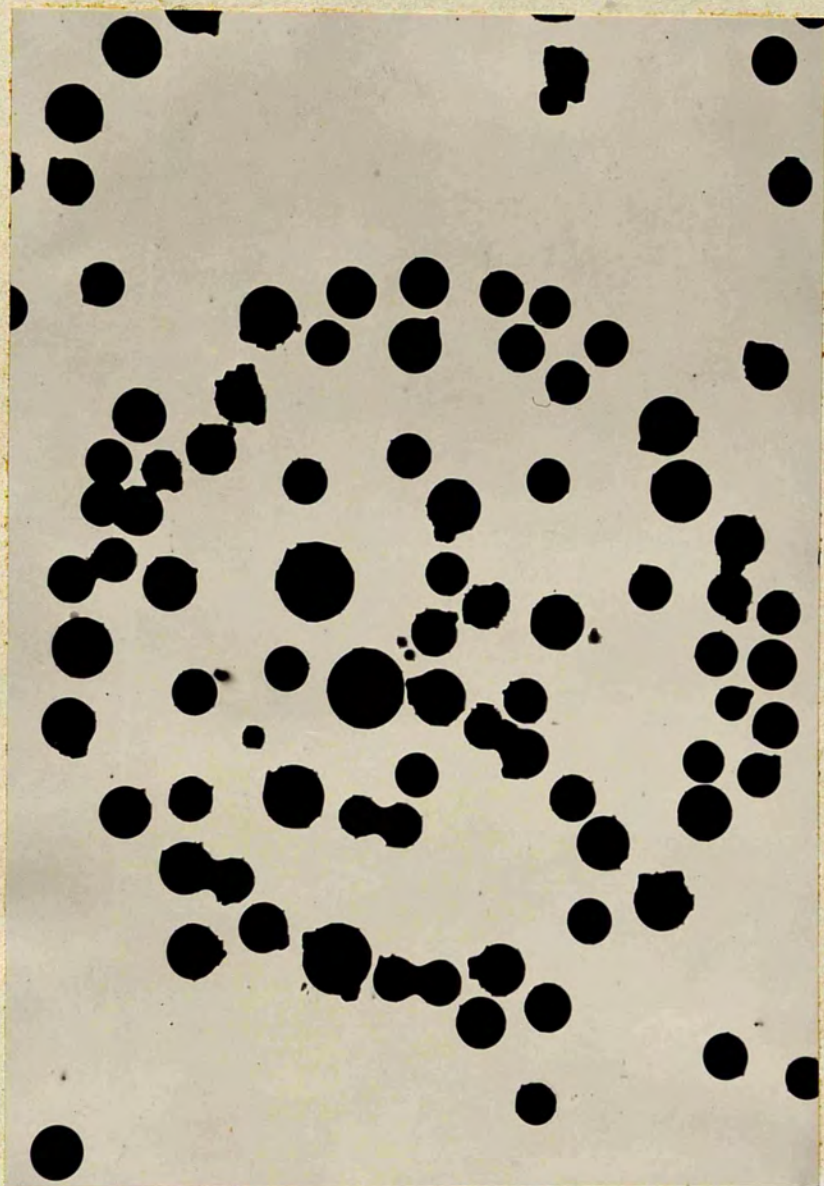


Figure 36. Selenium on polished (100) K Br.  $320\text{\AA}$   
mean thickness.  $\times 8000$ .



shows the opposite to be true.

Figure 36 shows a decoration feature similar to those described above, but at a higher magnification. The islands of selenium are seen to show great similarity with liquid droplets, being almost circular in shape. This resemblance is particularly striking where two islands are in the process of coalescing, and necking of the contact area typical of the joining of two liquid drops is shown in a number of cases. The diffraction pattern from such areas however shows all the features of a very well oriented crystalline deposit with no sign of amorphous material.

Unfortunately, with the equipment available it was impossible to determine whether at any stage the islands of selenium were in the amorphous or liquid state. Selenium in the vitreous state is relatively stable at room temperature, and has a softening point of about  $35^{\circ}\text{C}$ . It might therefore be possible for the liquid to exist as such for a short time at  $93^{\circ}\text{C}$  before crystallizing.

#### 4.4. Selenium films on polished (110) potassium bromide.

Potassium bromide single crystal cubes were cut and polished to reveal the (110) face using the method described in Chapter 3. The annealing temperature which gave the most suitable surface for epitaxial growth of the selenium



film was established by depositing films on surfaces annealed over a range of temperatures. Finally annealing at  $365^{\circ}\text{C}$  for one hour was found to produce the desired surface. Selenium was deposited on (110) surfaces prepared in the above way with the substrate temperature at  $96^{\circ}\text{C}$ , and the deposition rate at  $330\text{\AA}/\text{minute}$ . The mean thickness of the films was  $500\text{\AA}$ . This procedure produced oriented films of selenium which gave electron diffraction patterns of the spot type characteristic of good epitaxial growth.

Selenium films grown on potassium bromide crystals supplied by different companies did not however show the same microstructure, although the diffraction patterns from these films were very similar. Figure 37 shows two films grown on crystals from two different suppliers, under apparently identical conditions. In each case duplicate films were prepared to make certain that these two films were typical of the structure produced on each batch of crystals. Both microstructures were found to be reproducible.

The main differences between the microstructure shown in Figure 37(a) and Figure 37(b) appear to be the presence in 37(b) of the areas covered by a relatively thin film of selenium and the difference in the gross features of the thicker oriented areas. Diffraction patterns obtained from these films show that although the microstructure is

(a) analysis of the diffraction patterns.

different the orientation of the selenium is identical (Figures 38(a) and (b)).

The variation in properties of substrate crystals from different suppliers, and even from one batch to another from the same supplier has been noticed previously. Miller<sup>(95)</sup> found that although nickel can normally be grown epitaxially on cleaved and polished sodium chloride, some batches of crystals would not support epitaxial growth. Also the size of crystallites in films prepared under apparently identical conditions varied by a factor of five. The two types of crystals used as substrates were examined under crossed polaroids, and it was found that the type of crystal on which the film shown in Figure 37(b) was grown was very much more strained than that on which the film Figure 37(a) was grown.

It is difficult to draw any definite conclusions concerning the reason for the difference in microstructure of the two films, but it seems possible that differences in the detailed structure of the substrates are responsible. The making of large inorganic single crystals is as much an art as a science, and the details of preparation methods are trade secrets. Although both types of crystal were prepared from a melt the details of the methods are known to differ.

(a) Analysis of the diffraction pattern.





(a)



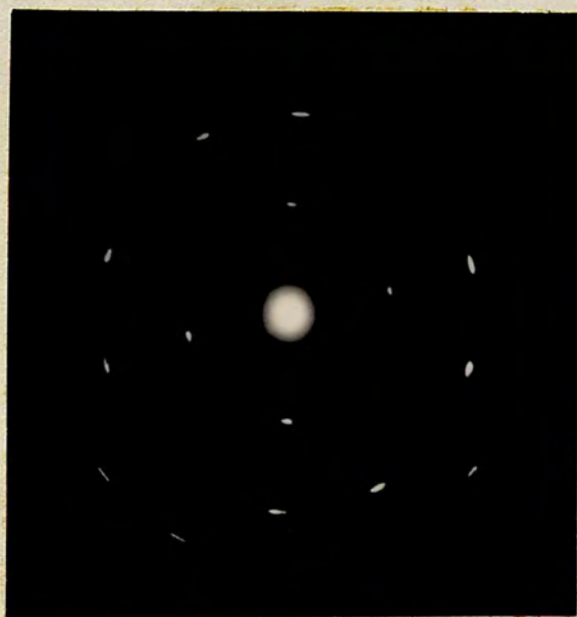
(b)

Figure 37. Selenium films on polished  
(110) potassium bromide.





(a)



(b)

Figure 38. Diffraction patterns from selenium films deposited on polished (110) potassium bromide.



The analysis of the diffraction pattern given by selenium deposited on (110) potassium bromide followed a similar course to that of the pattern given by selenium on (100) potassium bromide. Again the pattern did not correspond to any plane through the hexagonal selenium reciprocal lattice, and again it was found that it could be split into two identical superimposed primary patterns, this time at  $74^\circ$  to one another. This primary pattern was seen to be similar in form to the array of points obtained by taking a plane through the origin of the reciprocal lattice with zone axis  $11\bar{2}1$  (Figure 39). From this it follows that the selenium ( $11\bar{2}1$ ) plane was perpendicular to the electron beam, and oriented in two directions at  $74^\circ$  to one another. As the electron beam was perpendicular to the plane of the film it also follows that originally the selenium ( $11\bar{2}1$ ) plane was parallel with the substrate surface, and oriented in two directions at  $74^\circ$ . The diffraction pattern predicted from the reciprocal lattice for selenium oriented in this way (Figure 40) appeared to be almost identical with the experimentally observed pattern. Only one or two very faint spots due to small disoriented areas were not accounted for.

The positive identification of the selenium diffraction spots was again established by calibration with a superimposed sodium chloride pattern shown in Figure 41

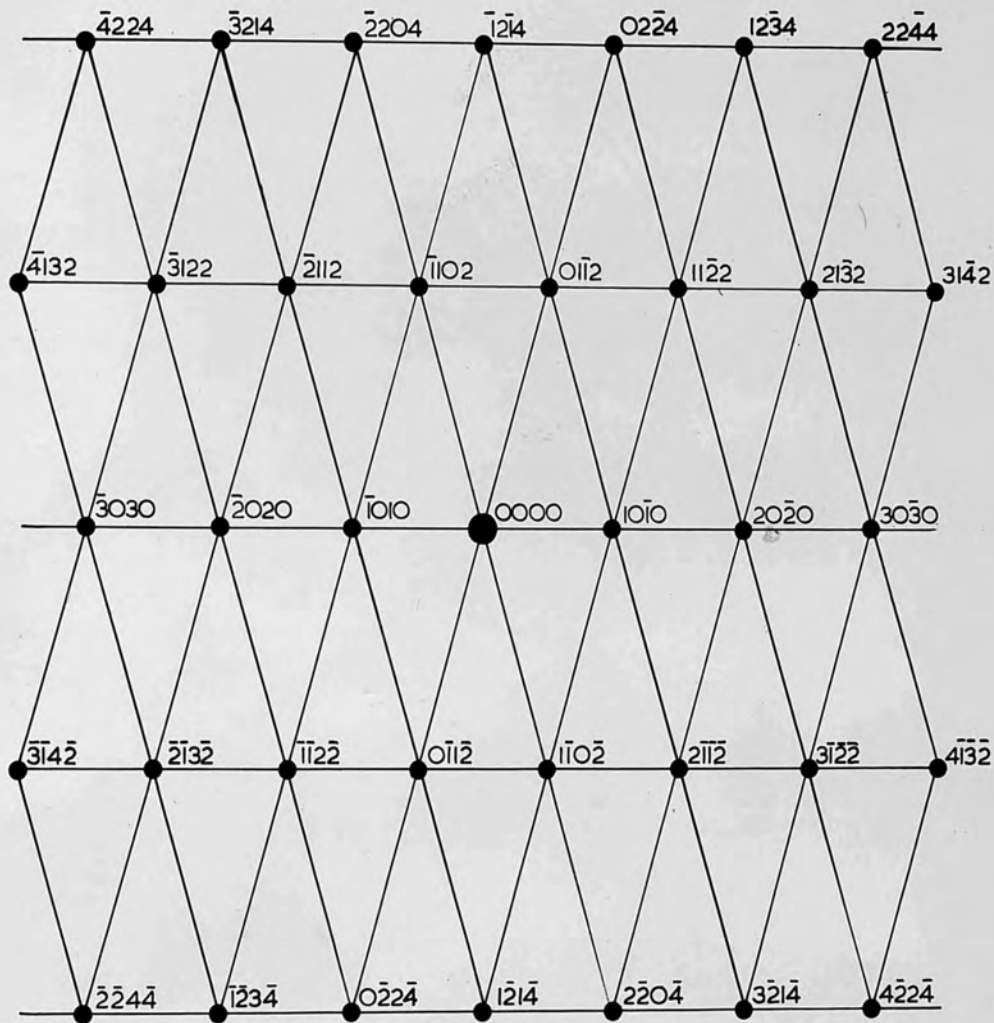
(see Chapter 4.1 and 4.3(a) for the method). Values of  $d$  calculated for the postulated  $10\bar{1}0$  and  $11\bar{0}2$  type reflections were  $3.76$  and  $2.06\text{\AA}$  respectively, compared with the actual values of  $3.7717$  and  $2.0691\text{\AA}$  respectively. This confirmed the original deductions concerning the origin of the diffraction pattern, and particularly that the selenium  $(11\bar{2}1)$  plane was parallel with the substrate surface.

(b) Orientation of selenium on the substrate.

The orientation of the selenium film with respect to that of the substrate was established using the method described in Chapter 4.1. In this case the substrate and the film were cleaved in the  $[001]$  substrate direction cutting the substrate face to give a straight reference edge to the film. This was again laid on the microscope grid with the straight edge parallel with the short sides of the grid apertures, and the combined diffraction pattern and shadowgraph of the grid bars produced in the electron microscope.

Figure 4.2. shows that the acute angle between the  $[10\bar{1}0]$  directions in the two orientations of the selenium  $(11\bar{2}1)$  plane was bisected by the substrate  $[110]$  type directions. This meant that the selenium  $(11\bar{2}1)$  face was parallel with the substrate  $(110)$  face, and the selenium  $[10\bar{1}0]$  directions in the two orientations of the





RECIPROCAL LATTICE FOR HEXAGONAL SELENIUM CRYSTAL:  
 PLANE THROUGH THE ORIGIN, WITH ZONE AXIS  $11\bar{2}1$

Figure 39.

102

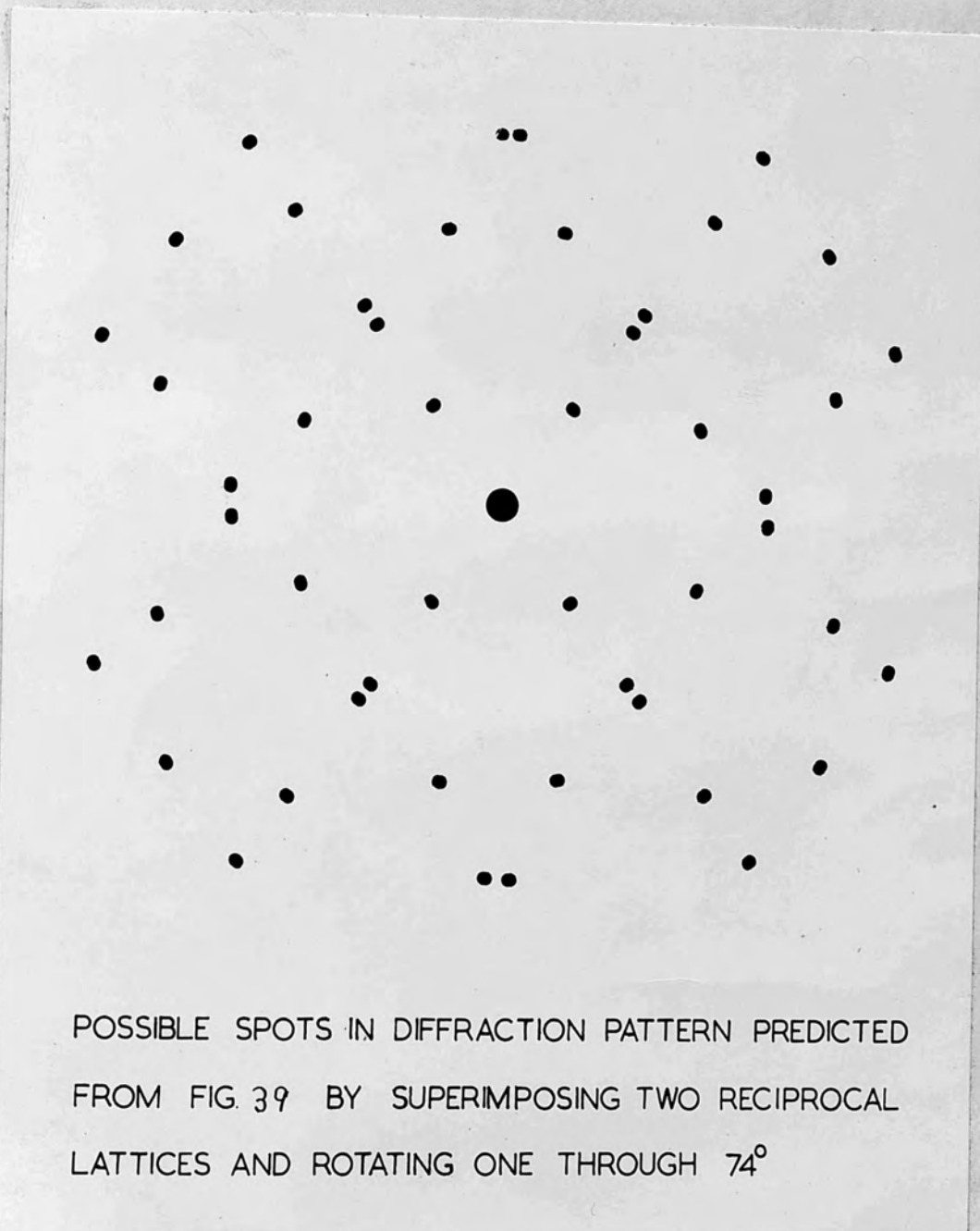


Figure 40.



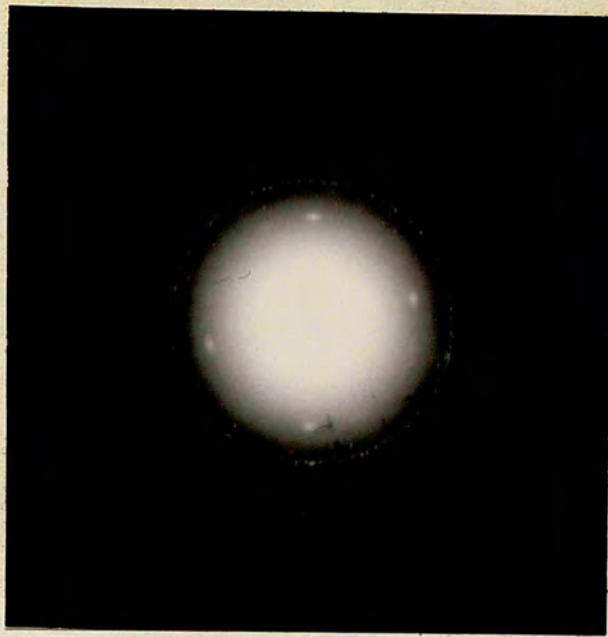


Figure 41. Diffraction pattern from selenium film with superimposed sodium chloride pattern.



Figure 42. Diffraction pattern from selenium film with superimposed grid bars.

(11 $\bar{2}$ 1) plane were at angles of  $37^\circ$  to, and either side of, the substrate [110] type directions.

#### 4.5. Selenium films on polished (111) potassium bromide.

Potassium bromide crystals were cut and polished to reveal the (111) face as described in Chapter 3. Selenium films were then deposited on such faces after annealing at  $365$ ,  $341$ , and  $316^\circ\text{C}$  for one hour. Annealing at  $365^\circ\text{C}$  was found to produce a face with very pronounced triangular etch features, but the other two annealing temperatures produced quite smooth surfaces. The films deposited on these surfaces at about  $96^\circ\text{C}$  with a deposition rate of about  $500\text{\AA}/\text{minute}$  showed no signs of epitaxial growth. Figures 43(a) and 43(b) show the micrograph and diffraction pattern of a typical film deposited at a substrate temperature of  $97^\circ\text{C}$ , with a mean thickness of  $900\text{\AA}$ .

The diffraction pattern is very similar to those given by selenium deposited on sodium chloride, the same rings being present in each. A diagram showing the indices of these rings is given in Figure 23.

#### 4.6. Selenium films on cleaved (111) calcium fluoride.

The calcium fluoride cleavage surfaces were first annealed at  $360^\circ\text{C}$  for one hour, and then films deposited at a substrate temperature of  $92^\circ\text{C}$  with a deposition rate of about  $500\text{\AA}/\text{minute}$ . Films produced under the above



conditions showed no tendency towards epitaxial growth. Figure 44. shows an electron micrograph and diffraction pattern from a typical film with a mean thickness of  $700\text{\AA}$ . The diffraction pattern is again similar to that from films deposited on sodium chloride which are indexed in Figure 23.

#### 4.7. Selenium films on cleaved (111) barium fluoride.

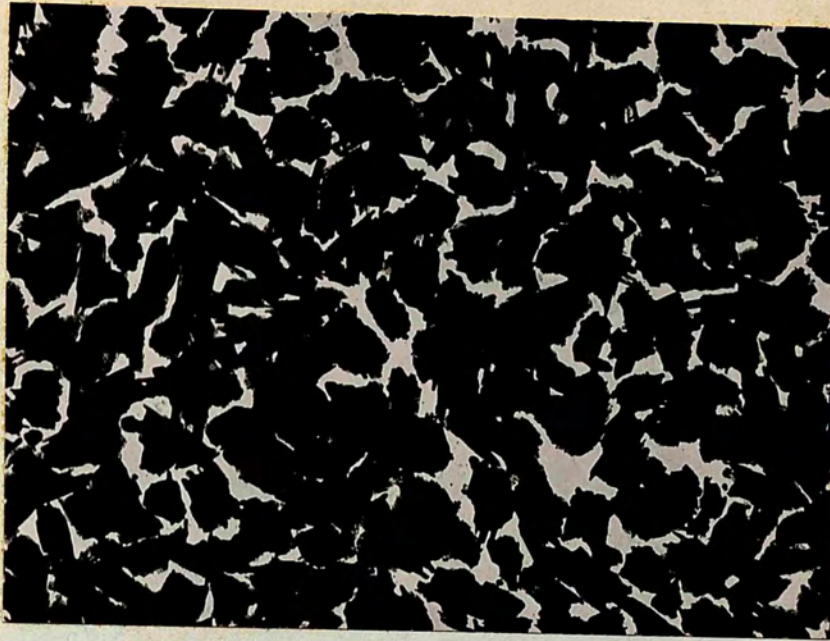
Barium fluoride cleavage surfaces were annealed for one hour at  $340^{\circ}\text{C}$  and then the film was deposited. It was found that at the evaporation rate used no film deposited on the substrate at  $93^{\circ}\text{C}$ . The substrate temperature was therefore reduced to  $88^{\circ}\text{C}$ . Films were deposited at this temperature with a deposition rate of  $500\text{\AA}/\text{minute}$  to give a mean film thickness of  $700\text{\AA}$ . Again no tendency towards epitaxial growth was observed. Small oriented areas gave non uniform diffraction rings but this orientation was not consistent in direction from one area to another. The structure of the films and the diffraction patterns were very similar to those of films deposited on calcium fluoride. Figure 45 shows the electron micrograph, and diffraction pattern from a typical film.

#### 4.8. Selenium films on cleaved (100) magnesium oxide.

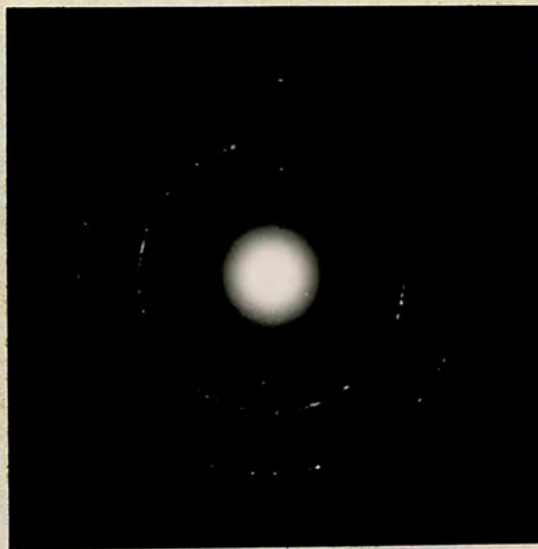
Selenium had previously been deposited on cleaved magnesium oxide at  $112^{\circ}\text{C}$  by Schossberger. He observed in the film only a small amount of unoriented hexagonal

selenium, together with an unknown phase giving two broad diffraction rings, presumably amorphous selenium. Selenium was therefor deposited at a lower substrate temperature,  $88^{\circ}\text{C}$ , which was known to give epitaxial growth with potassium bromide. The magnesium oxide was annealed at  $425^{\circ}\text{C}$ , and the selenium deposited to give a mean film thickness of  $600\text{\AA}$  at a deposition rate of  $400\text{\AA}/\text{minute}$ . Films prepared in this way showed no signs of epitaxial growth, and were mostly amorphous. Figure 46(a) shows the micrograph of a film with small crystalline areas and amorphous islands. The diffraction pattern, Figure 46(b) shows the superimposed amorphous patterns of the selenium and the carbon support film.





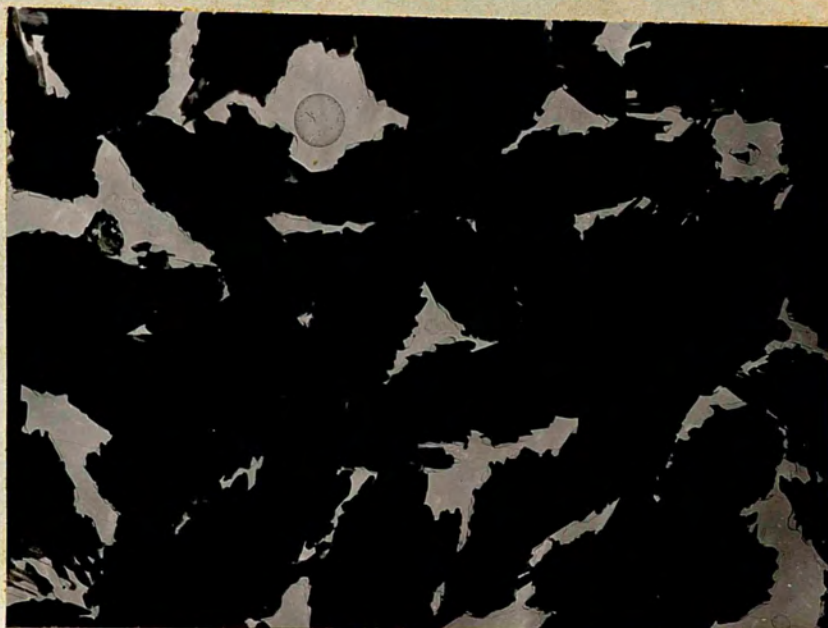
(a) Electron micrograph. x 8000.



(b) Diffraction pattern.

Figure 43. Selenium deposited on polished (111) potassium bromide.





(a) Electron micrograph. x 8000.



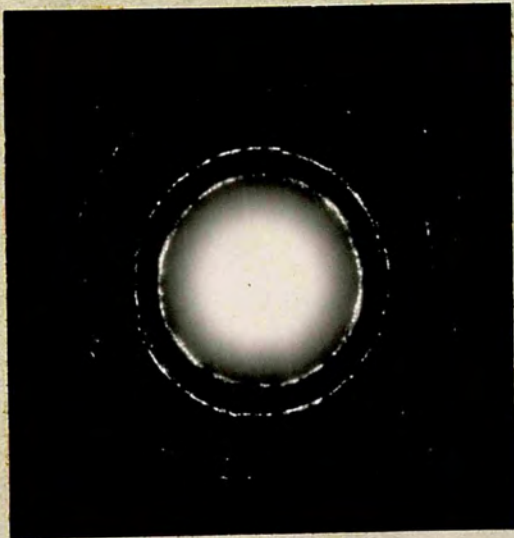
(b) Diffraction pattern.

Figure 44. Selenium deposited on cleaved (111) calcium fluoride.





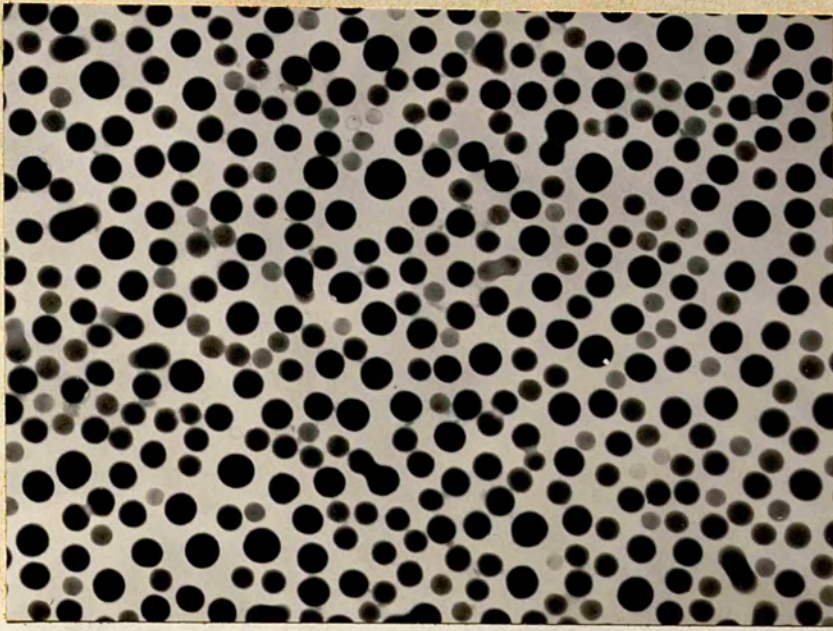
(a) Electron micrograph. x 8000.



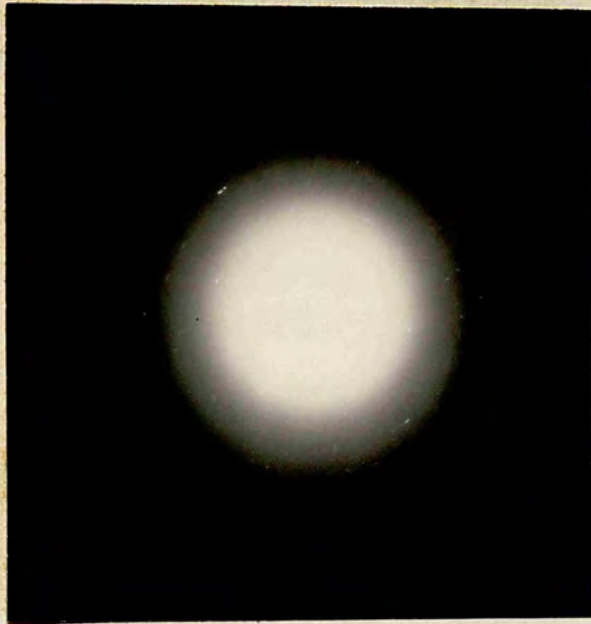
(b) Diffraction pattern.

Figure 45. Selenium deposited on cleaved (111) barium fluoride.





(a) Electron micrograph. x 8000.



(b) Diffraction pattern.

Figure 46. Selenium deposited on cleaved (100) magnesium oxide.



References to Chapter 4

95. Miller, R.F., Private communication

## Chapter 5. Determination of film thickness.

### 5.1. Introduction.

The selenium films described in chapter 4 were continuous only at thicknesses which rendered them electron opaque, and so precluded any determination of structure. Nevertheless it was thought useful to attempt determinations of thickness of a range of films up to this thickness.

A method capable of giving actual film thicknesses to a high degree of accuracy is the multiple beam Fizeau fringe technique (Tolansky 1948)<sup>92</sup>. This method has been used in a number of cases for films on glass, but unfortunately proved impracticable with selenium. The silver layer required for high reflectivity of the surface was found to react with selenium at room temperature to give a poorly reflecting matt surface. No fringes could be obtained from the selenium, although good fringes were obtained from the substrate. The method finally used involved the chemical determination of the selenium present on the substrate surface. Assuming the film to possess bulk density the mean thickness over the 1 c.m. diameter film was calculated from the mass of selenium and its area.

50 ml. aliquots of this solution were then reacted with 2 ml. of a 0.5% aqueous solution of 5,5'-diaminobenzidine for



## 5.2. Fluorimetric determination of Selenium.

Chemical determinations of selenium were done with the help of Rank Xerox Ltd., who use a similar method for the determination of selenium in solutions. This method is basically that developed by Watkinson (1960)<sup>96</sup> for the analysis of selenium in vegetable matter, in which the fluorescence of the selenadiazole formed from 3,3'-diaminobenzidine is measured. Due to the fact that the only foreign elements present were potassium, and possibly tin from the stannic oxide polishing media, no elimination of interfering elements were necessary.

The selenium film on its substrate was digested in 1 ml. of nitric acid in a borosilicate glass tube, and the evolved bromine led off and absorbed. Nitric acid was added drop wise until the solution became colourless. The solution was evaporated to incipient dryness and the residue dissolved in two drops of nitric acid, and distilled water. Care was taken during the evaporation procedure not to heat too strongly, as this was found to cause evaporation of selenium dioxide. The solution was made up to 250 ml. with distilled water, the pH being adjusted to 2.5 (Meta cresol purple indicator) by the addition of ammonium hydroxide or formic acid. 50 ml. aliquots of this solution were then reacted with 2 ml. of a 0.5% aqueous solution of 3,3'-diaminobenzidine for

30 minutes, neutralized, and the selenadiazole extracted with 25 ml. of toluene. The toluene was then separated and dried over sodium sulphate.

The determination of selenium was made in a "Hilger and Watts H.960. Fluorimeter". Light from a mercury arc lamp passed through a "Wratten 47" filter (370 to 520  $m\mu$ ) was used to irradiate the selenadiazole. Excitation caused by the mercury 405 and 436  $m\mu$  lines produced fluorescence at 580  $m\mu$  which was isolated with a sodium interference filter (589  $m\mu$ ) and measured with a photocell in series with a galvanometer. Fluorescence was compared with that of standard selenium solutions prepared in the same manner, and also with solutions to which potassium bromide had been added.

The selenium present was calculated after allowances had been made for the fluorescence of the blank solution and interference by the potassium nitrate present.



### References to Chapter 5.

96. Watkinson, J.H. (1960). Analytical Chemistry. 32, 981.

Chapter 6. Discussion of results, and future work.

6.1. Discussion of results.

The results given in Chapter 4 show that selenium will grow epitaxially on certain ionic substrates, although it is not obvious why epitaxy should occur on some substrates and not on others. Only one factor stands out, and that is the small misfit of substrate and overgrowth where epitaxy has occurred. In the case of selenium on (100) potassium bromide the misfit along the [110] type directions in the (100) face is 5%. With selenium on (110) potassium bromide the misfit along the [001] substrate direction is less than 1%, and along the [110] substrate direction is less than 1% for a multiple of two substrate unit cells. The misfits for selenium in similar orientations on (100) and (110) sodium chloride would be 8.5% for the (100) face, and 17% along the [001] direction in the (110) face. No epitaxial growth occurred on either the potassium bromide or sodium chloride (111) faces where the misfit of the selenium basal plane would be -7% and + 9.5% respectively.

The other substrate with a sodium chloride type structure was magnesium oxide. Taking misfit as a factor governing the tendency towards epitaxial growth, one might expect the orientation of the selenium (1010) plane parallel to the substrate (100) face, with the selenium



C axis parallel with magnesium oxide cube edge (misfit 4%). However in this case the behaviour of the deposited film was different from that of films on the other substrates with the same structure. It seems rather unusual that the film should be largely amorphous at a substrate temperature which gave perfectly crystalline films on other substrates. The same behaviour was however found by Schossberger<sup>47</sup> in similar selenium evaporations onto this substrate.

Selenium was also deposited on the (111) cleaved faces of calcium and barium fluoride with no sign of epitaxial growth, even though the misfit of the selenium (0001) plane on the (111) barium fluoride surface is only -0.4% (+ 13% on calcium fluoride).

On the basis of the selenium films prepared on the above substrates it seems that although misfit might have some influence on the tendency towards epitaxial growth of selenium, other factors must also have a large influence. Among these factors must be the effect of adsorbed gases on the substrate surface, in that taking up preferred sites themselves, the adsorbed gas molecules must seriously modify the substrate surface properties.

Lander, Gobeli, and Morrison (1963)<sup>97</sup> have recently examined the (111) cleavage face of silicon and germanium using slow electron diffraction. They found that this

surface did not exhibit the three fold symmetry of atomic array which would be expected from the bulk structure of the crystal, but rather a rectangular array. This was formed by large displacements of the surface layer, and second layer atoms from their original sites, and could be altered by heat treatment to produce other structures.

It would seem therefore that with these crystals, and probably others, details of surface structure cannot be predicted with any certainty from the bulk form of the crystal. This throws some doubt on the value of calculated misfits for the growth of one crystal lattice upon another. Any correlation between misfit and epitaxial growth must be made on the basis of the actual atomic arrays at the plane of contact.

Notwithstanding the reservations expressed concerning the value of misfit calculations, misfit diagrams for selenium in the observed double orientations on (100) and (110) potassium bromide were drawn. In each case the selenium atoms in the planes of contact are arbitrarily placed over the potassium ions, and the two lattice nets of the double orientations are shown superimposed.

This superimposition of the lattice nets is not meant to indicate that the film has this structure, but rather to

preparing single crystal films of the element.



indicate the two orientations found in separate selenium crystallites.

It can be seen from Figure 47 that the fit of the selenium  $(10\bar{1}0)$  plane on the potassium bromide  $(100)$  plane is very good and that this fit extends over a number of unit cells. In this case the selenium chains are lying parallel to the substrate, with every third atom along the chain in the  $(10\bar{1}0)$  plane (Figure 48). Selenium on  $(110)$  potassium bromide (Figure 49) again shows good fit of the lattice planes, particularly every two unit cells in the substrate  $[\bar{1}10]$  direction. It is rather interesting to find that although theoretically there would be even less misfit if the selenium lattice was rotated through  $2^\circ$  to bring the selenium atoms directly above the potassium ions in substrate  $[001]$  direction, this does not in fact occur.

Although some doubt has recently been thrown on the value of apparent lattice misfit as an explanation of epitaxial growth, the orientation of selenium on  $(100)$  and  $(110)$  potassium bromide is that which conforms to the condition of least misfit.

## 6.2. Future work.

The experiments which have been performed have shown that it is possible to prepare epitaxially grown films of selenium. They have also indicated the possibility of preparing single crystal films of the element.

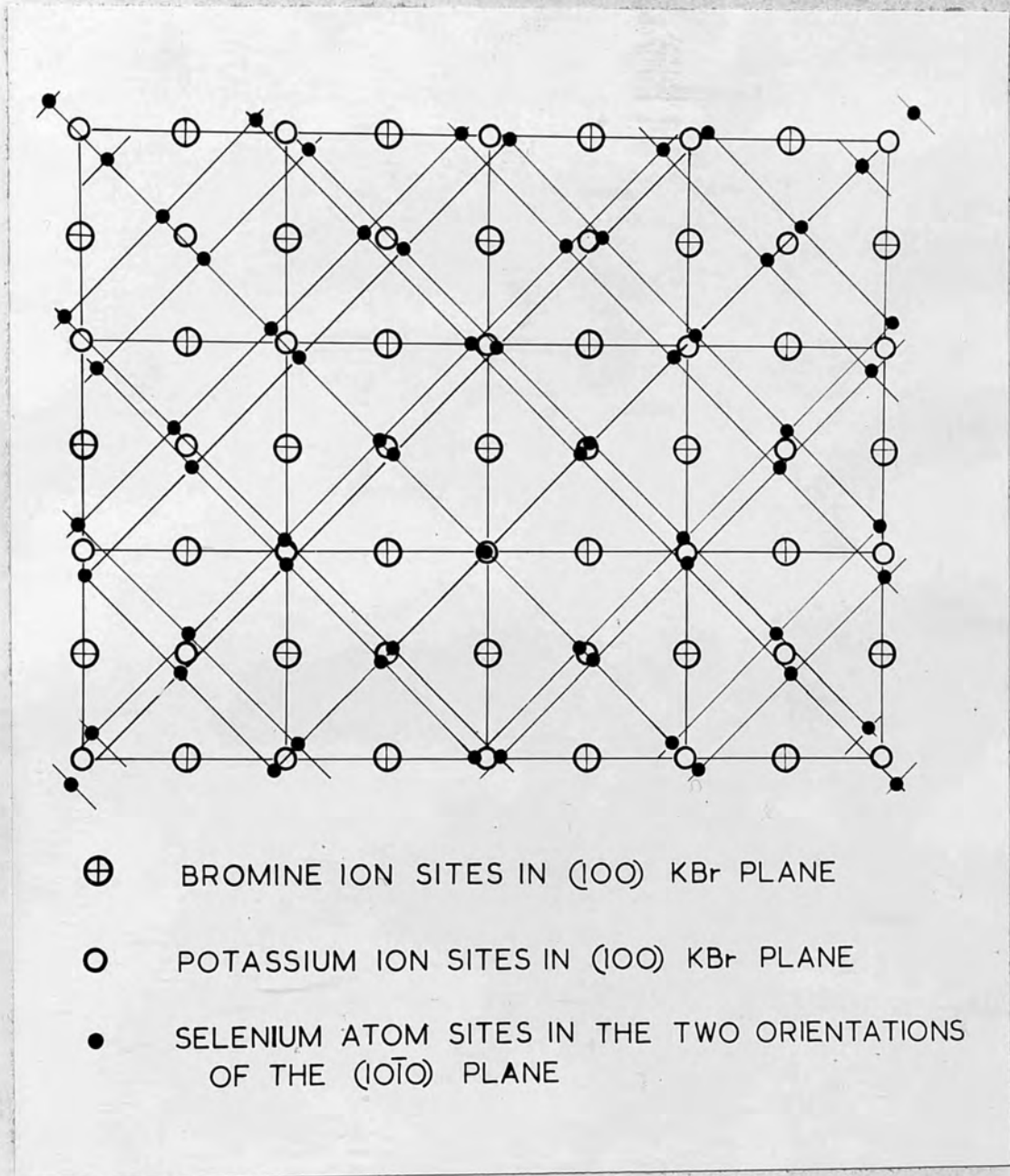


Figure 47.



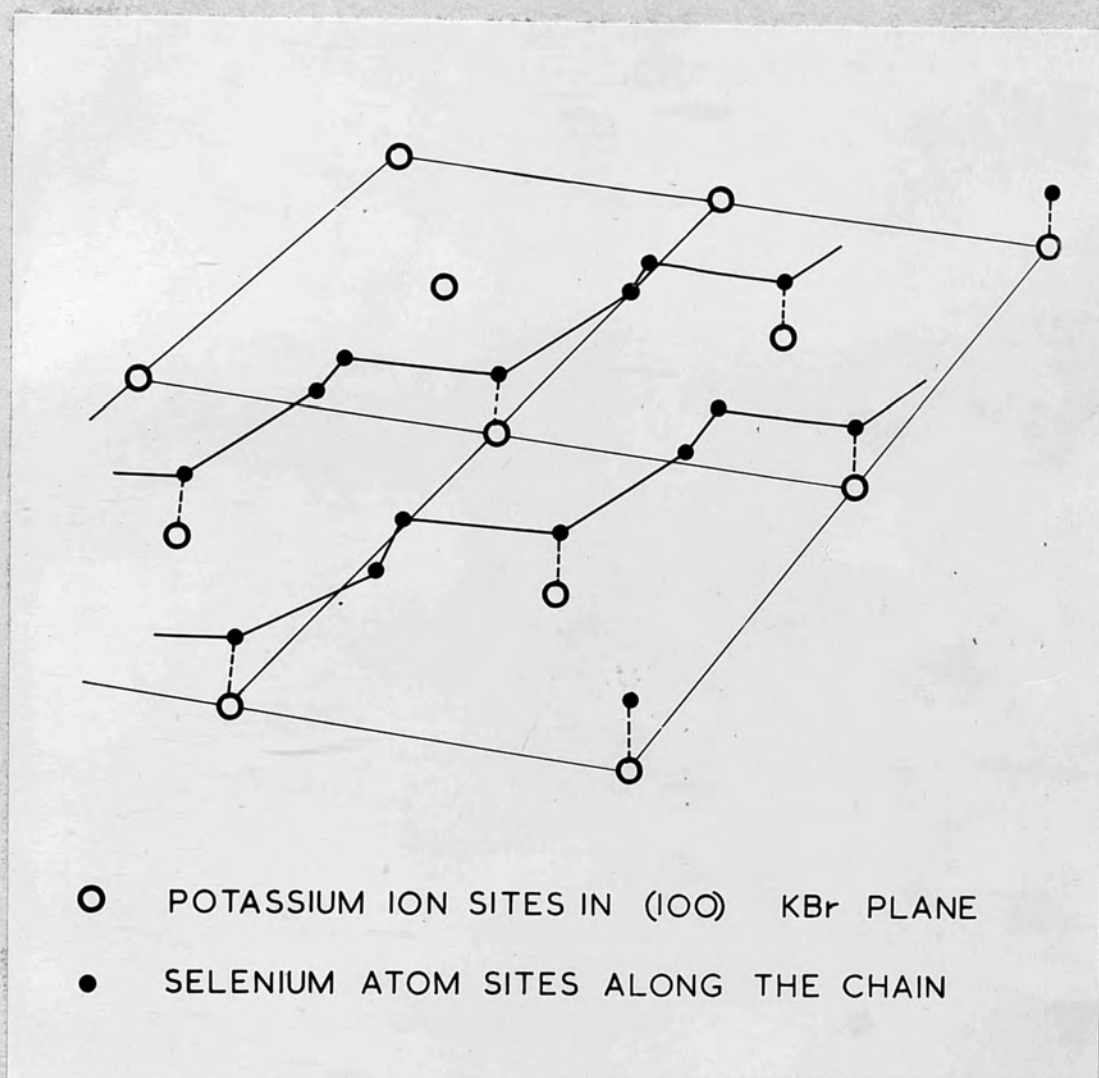
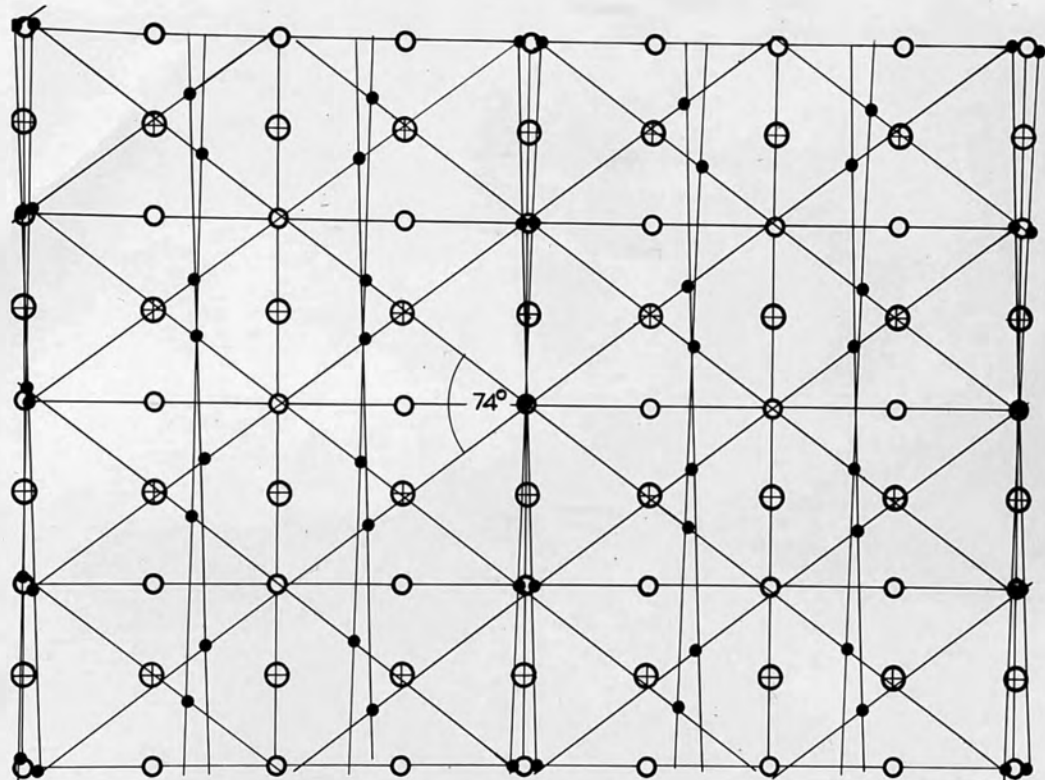


Figure 48.



- $\oplus$  BROMINE ION SITES IN (110)  $\text{KBr}$  PLANE
- $\circ$  POTASSIUM ION SITES IN (110)  $\text{KBr}$  PLANE
- $\bullet$  SELENIUM ATOM SITES IN THE TWO ORIENTATIONS OF THE  $(1\bar{1}2)$   $\text{Se}$  PLANE

Figure 49.



Such single crystal films would be ideal specimens on which to measure the electrical properties of selenium under clean and controlled conditions. It would be desirable therefore to extend the range of substrates used, in order to develop methods of preparing single crystal films with various orientations of the C axis with respect to the plane of the film. Although the growth of selenium films on previously epitaxied metal films might be difficult, due to the reactivity of selenium, it might be possible in this way to induce the selenium films to become continuous at lower thicknesses. This would allow a more detailed examination of the film structure.

Recent work on epitaxial growth, and single crystal surfaces, has shown the importance of the cleanliness of the substrate surface. It has also shown that for any correlation to be made between the structure of the substrate and over growth, the actual atomic array on the substrate surface should be known. Simultaneous cleavage of the substrate and film deposition under ultra high vacuum ( $10^{-8}$  mm./Hg. or better) would decrease the chances of the substrate surface becoming contaminated. The use of pumping systems which do not employ oil or mercury would also reduce the contamination due to the backstreaming of these working fluids.

An examination of the substrate surface by slow electron diffraction would allow the type of atomic array

on the surface to be known with some accuracy. It would also allow a better evaluation of the importance of misfit in epitaxial growth.

The process of stripping the film from the substrate for examination must introduce some degree of disorientation. This would be avoided by the use of reflection electron micrography and diffraction in the examination of the film while still on the substrate. Still more information could be obtained if a combined vacuum evaporation plant and electron microscope was available.



References to Chapter 6

97. Lander J.J., Gobel, G.W., and Morrison, J.,  
(1963) J. Appl. Phys., 34, 2298.